Healthcare Analytics 5 (2024) 100308

Contents lists available at ScienceDirect

Healthcare Analytics

journal homepage: www.elsevier.com/locate/health

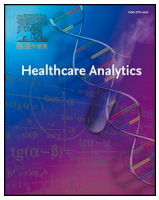

A computational fractional order model for optimal control of wearable healthcare monitoring devices for maternal health

Onuora Ogechukwu Nneka [a], Kennedy Chinedu Okafor [b,*], Christopher A. Nwabueze [a], Chimaihe B Mbachu [a], J.P. Iloh [a], Titus Ifeanyi Chinebu [c], Bamidele Adebisi [b], Okoronkwo Chukwunenye Anthony [b,d]

[a] Department of Electrical Electronic Engineering, Chukwuemeka Odumegwu Ojukwu University, Uli, Anambra State, Nigeria
[b] School of Engineering, Manchester Metropolitan University, Manchester, M1 5GD, UK
[c] Federal College of Dental Technology and Therapy, Trans - Ekulu, Enugu, 400281, Nigeria
[d] Department of Mechatronics Engineering, Federal University of Technology, Owerri, NG 1526, Nigeria

ARTICLE INFO

Handling Editor: Madijd Tavana

Keywords:
Computational intelligence
Fractional order model
Optimal control
Wearable healthcare monitoring device
Differential transform model

ABSTRACT

The post-COVID-19 landscape has propelled the global telemedicine sector to a projected valuation of USD 91.2 billion by 2022, with a remarkable compounded annual growth rate (CAGR) of 18.6% from 2023 to 2030. This paper introduces an analytical wearable healthcare monitoring device (WHMD) designed for the timely detection and seamless transmission of crucial health vitals to telemedical cloud agents. The fractional order modeling approach is employed to delineate the efficacy of the WHMD in pregnancy-related contexts. The Caputo fractional calculus framework is harnessed to show the device potential in capturing and communicating vital health data to medical experts precisely at the cloud layer. Our formulation establishes the fractional order model's positivity, existence, and uniqueness, substantiating its mathematical validity. The investigation comprises two major equilibrium points: the disease-free equilibrium and the equilibrium accounting for disease presence, both interconnected with the WHMD. The paper explores the impact of integrating the WHMD during pregnancy cycles. Analytical findings show that the basic reproduction number remains below unity, showing the WHMD efficacy in mitigating health complications. Furthermore, the fractional multi-stage differential transform method (FMSDTM) facilitates optimal control scenarios involving WHMD utilisation among pregnant patients. The proposed approach exhibits robustness and conclusively elucidates the dynamic potential of WHMD in supporting maternal health and disease control throughout pregnancy. This paper significantly contributes to the evolving landscape of analytical wearable healthcare research, highlighting the critical role of WHMDs in safeguarding maternal well-being and mitigating disease risks in edge reconfigurable health architectures.

1. Introduction

Reconfigurable device architectures for emerging health systems require new computational models for health analytics. Wearable Healthcare Monitoring Device (WHMD) represents an edge telemetry innovation designed for non-intrusive placement on the user's body. This device operates as an actionable standard for monitoring pertinent health indicators. Positioned on the wrist or other body locations, WHMD leverages biosensors to collect diverse physiological data such as heart rate, blood pressure, sleep patterns, and physical activity [1]. These biosensor devices may capture data via non-invasive physiological tracking or minimally invasive substrate sensing methods. The direct detection of specific bodily substrates by biosensors offers supplementary risk stratification information, circumventing delays and costs associated with traditional laboratory procedures. A typical application is the Google Fit and Samsung app, etc. These applications highlight the variety of ways that technology can be applied to real-time health monitoring and improvement.

A computational model for real-time tracking of user activity and health data could facilitate seamless data transmission to healthcare

* Corresponding author.
E-mail addresses: ogeonuora@gmail.com (O.O. Nneka), k.okafor@mmu.ac.uk (K.C. Okafor), canwabueze09@gmail.com (C.A. Nwabueze), dambac614@gmail.com (C.B. Mbachu), titusifeanyi5432@gmail.com (T.I. Chinebu), b.adebisi@mmu.ac.uk (B. Adebisi), chukwunenye.okoronkwo@futo.edu.ng (O. Chukwunenye Anthony).

https://doi.org/10.1016/j.health.2024.100308
Received 8 November 2023; Received in revised form 23 December 2023; Accepted 2 February 2024
Available online 11 February 2024

professionals and physicians [2]. This dynamic interaction enables clinicians to gain deeper insights into patient well-being and disease management. This aggregated data sharing among multiple patients to a centralized point optimizes resource allocation and timeliness by enabling early identification of illness.

Globally, the healthcare and wellness sector has continued show growing trend towards personalized and monitored healthcare, driven by advancements in mobile technology [3]. Contemporary tools like artificial intelligence [4], robots [5], smart sensors [6], big data analytics [7], and digital wearables [8] play pivotal roles in disease prevention and management. These technologies facilitate the estimation of key parameters like blood pressure, body temperature, heart rate, and respiration, enabling the early detection of health deterioration, disease exacerbation, and critical events such as spikes in blood pressure or respiratory issues [9].

Pregnancy, being a sensitive phase for both the mother and fetus, demands meticulous health monitoring. As such, wearable devices tailored for expectant mothers offer continuous monitoring over extended periods, transmitting real-time insights to healthcare providers [10]. These wearables enhance maternal health by promptly identifying health deviations and enabling data sharing with medical professionals.

This shared data empowers care providers to recommend specific interventions for improved health outcomes. There are various ways proposed for wearable telemedicine such as data-driven telemedicine [11–13].

Computational operators like fractional differential operators have recently been applied in health modeling [14,15]. Traditional operators like the Newtonian and Riemann-Liouville fractional cannot explain complicated real-world problems like pregnancy telemedicine [16]. However, these new operators have shown promise and are likely to become a crucial part of solving real-world problems. This because of its ability to allow mathematical models consider long-term connections caused by memory resources.

Till date, most computational models represent these real-world scenarios [17–19]. The use of fractional dynamics and nonlocal nature of fractional order models enhances predictive accuracy for physical systems [9,10]. Because fractional models accurately represent non-integer order kinetics, it is a valuable tool in the modeling of complicated health systems [20]. It helps establish long-term dependencies in health-related processes by introducing memory into mathematical models [21]. Fractional order controllers are used in medical equipment to improve control efficiency, particularly in systems that are naturally complicated. For instance, such models improve the design of drug delivery devices by enabling more precise predictions and optimization [21]. Fractional model non-locality helps analyze complex vital signals. It provides a sophisticated explanation of physiological parameter changes over time, making it an invaluable tool for researching antenatal and degenerative processes [23]. Its use in biomedical imaging improves the precision of diagnosis and image quality [24]. Fractional model is useful in the field of disease progression modeling [25]. Its fractional order derivatives and non-local dynamics give more accurate predictive models.

In this context, the differential transform method (DTM) [25] provides approximate solutions for linear and nonlinear problems in most complex design analysis. Employing the Caputo fractional operator enhances model realism by incorporating traditional initial values and considering interactions with past information [26,27]. Fractional calculus accommodates non-integer derivatives, often nonlocal, in modeling real-world problems.

This study employs a six-compartmental fractional order Caputo model to leverage wearable healthcare devices designed monitoring pregnant patient health. This approach capitalizes on the efficiency of the Caputo fractional operator.

The paper is structured as follows. Section 2 covers preliminary aspects and model formulation, transitioning from classical derivatives to non-classical orders using the Caputo approach. Section 3 presents quantitative findings for the fractional order model, encompassing equilibrium solutions, the basic reproduction number, and sensitivity analysis thereof concerning wearables. Section 4 addresses optimal control of the fractional order problem, while Section 5 delves into numerical solutions of model variables via the Fractional Multi-Stage Differential Transform Method (FMSDTM) [28]. Numerical simulations and their discussions are provided in Section 6, culminating in conclusions in Section 7.

1.1. Problem statement

This paper has highlighted five potential problem statements in respect of maternal health monitoring:

- Inadequate Maternal Health Monitoring during Pregnancy: In Ref. [29], the existing healthcare monitoring methods lack continuous and real-time tracking capabilities, leading to potential delays in detecting and addressing health issues in pregnant individuals.
- Optimal Integration of Wearable Devices in Maternal Care: This the challenge lies in determining the most effective ways to integrate such devices into the prenatal care routine to ensure timely detection of health deviations and appropriate medical interventions.
- Modeling the Efficacy of Wearable Devices in Disease Control: A model that accurately represents the impact of wearable healthcare devices on disease prevention and management during pregnancy is useful.
- Fractional order healthcare Dynamics: Using fractional order to model healthcare dynamics innovative.
- Implementing Optimal Control Strategies for Maternal Health: Identifying and implementing optimal control strategies using wearable devices during pregnancy require overcoming challenges related to data interpretation, decision-making, and resource allocation for effective maternal care.

In this paper, four contributions are highlighted, and these demonstrate an innovative approach to using fractional calculus and wearable healthcare devices in the context of maternal care and telemedicine. These contributions:

- Transition to Fractional Calculus: We establish a novel transition from classical derivatives to non-classical orders using the Caputo approach.
- Fractional Order Model for Maternal Health Monitoring: We derive a fractional order model for monitoring the health of pregnant women using WHMDs. This modeling approach represents a novel contribution to the field of telemedicine and maternal care.
- Optimal Control Strategies are identified for maternal health using WHMDs. This will explore the use of data interpretation, decision-making, and resource allocation.
- Numerical Solutions with FMSDTM: The paper utilise the Fractional Multi-Stage Differential Transform Method (FMSDTM) to numerically solve the fractional order model.

2. Telemedicine edge preliminaries and antenatal model formulation

In this section, fractional derivatives used to consider a pregnant patient with health complications. Let's start with baseline preliminaries in Section 2.1.

2.1. Preliminaries

Definition 2.1. LI and Ma, [30]; Ogunmiloro [28], the Riemann – Lioville integral of order $\varepsilon > 0$ of function $f(t)$ is defined by the integral

$$D^{\varepsilon}_{0,t}f(t) = \frac{1}{\Gamma(\varepsilon)\int_0^t (t-\vartheta)^{\varepsilon-1} f(\vartheta)d\vartheta} \quad t > 0 \tag{1}$$

Definition 2.2. Alkhudhari et *al*, [31]; Ogunmiloro et al. [32], Given a well-defined continuous function $f(t) \in C^n[0, t_f]$ *with* $\varepsilon > 0$, the Caputo fractional derivative of $f(t)$is defined by

$${}^{C}_{a}D^{\varepsilon}_{0,t}f(t) = \frac{1}{\Gamma(n-\varepsilon)\int_0^t (t-\vartheta)^{n-\varepsilon-1} f^n(\vartheta)d\vartheta}, \textit{where } n-1 < \varepsilon \leq n \tag{2}$$

$n \in N$, such that if $\varepsilon \to 1$, then ${}^{C}_{a}D^{\varepsilon}_{0,t}f(t) \to f^{(t)}$ *if* $t \in (0,1)$, *then* one obtains Equ (3)

$${}^{C}_{a}D^{\varepsilon}_{0,t}f(t) = \frac{1}{\Gamma(n-\varepsilon)}\int_0^t \frac{f^n(\vartheta)}{(\varepsilon-\vartheta)^t}d\vartheta \tag{3}$$

2.2. Edge model formulation

This Section discussed the edge layer of the telemedicine infrastructure and presented a comprehensive model. We aimed at monitoring the health status of pregnant women through the utilisation of Healthcare Sensory Device Intelligence (HSDI). Introducing specialized compartments (referred to as Classes) within this model serves the purpose of clearly delineating both the pregnant women under observation and the populace of wearable healthcare devices (WHMD). The model is governed by the following assumptions.

1. There is no immigration of infected pregnant women.
2. The total pregnant women population $N(t)$ is constant.
3. The coefficient of transmission of diseases is constant and does not vary with diseases.
4. After given birth, the women are no more pregnant, and leave the population under study at a rate μ_g and this is equal in all classes.
5. Death is neglected, as the period of pregnancy is nine months (about 40 weeks) which is much smaller than the mean lifespan of humans.
6. Pregnant women are assumed to be put on wearable healthcare monitoring devices during pregnancy.
7. Recovered pregnant women after medical consultation and treatment return to the susceptible class due to weak immunity at a rate φ.
8. Susceptible pregnancy after normal medical consultation due to data transmitted from the wearables return to susceptible class at a rate ξ.
9. The wearable devices collect the health data of pregnant women and share it with the healthcare provider or qualified doctors.
10. The Cloud healthcare provider immediately utilizes the data received from the edge to make decisions about specific measures that can improve pregnant women's health status.

2.3. Parameters and variables

This subsection provides and explains the parameters as well as the variables that describe the model for monitoring pregnant women's health using WHMDs. Table 1 shows the description of Parameters for wearable Telemedicine device.

Table 1
Description of Parameters for wearable telemedicine device.

Parameters	Description
ψ	Recruitment rate of susceptible pregnant women with wearable device
ξ	The rate movement of pregnant women with wearables who after normal consultation with the healthcare providers return to the susceptible class
φ	The rate at which the recovered pregnant women with wearables move to the susceptible class because of impaired immune function
$\alpha, \gamma, \varnothing$	The rate at which the biosensor of the wearable devices collect data from susceptible, exposed, and infected pregnant women with wearables respectively
η	Modified parameter that accounts for the rate at which data collected from the exposed and infected pregnant women are shared with the healthcare provider
τ, τ_1, τ_2	The rate of movement of susceptible, exposed, and infected pregnant women with wearables respectively to consultation and treatment class
β	The rate at which susceptible pregnant women with wearables become exposed to diseases or infections
μ_g	The rate at which women leave the population under study after delivery because such patient is no longer pregnant
ρ	Persistent use of wearable devices
d	Death due to pregnancy complications
σ	Rate at which exposed pregnant women with wearable can become infectious
Λ	The rate constant at which the exposed may recover
π	The effective data transmission rate
υ	The rate constant at which the Monitored and Treated Pregnant Women with wearables recover
κ	The energy of the wearable devices
Λ	The identification of infection
h	Is infirmaries of identification
P	Is pregnant women with different type of diseases or infections
δ	Is the work functionality of the device
t	Time

However, for large classes, it is more realistic to consider the wearables that do not depend on the total population but on their fraction (individual classes) with respect to the total population $N(t)$. Now, let's consider that

$$\lambda = \pi(S + \eta(E+I)) \tag{4}$$

Where λ is the force of sharing data associated with pregnant women's health using wearable devices with healthcare providers. π is the effective data transmission rate, that is the rate at which the wearables after detecting health imbalances of pregnant women-share them with healthcare providers. The modified parameter η accounts for the rate at which data collected from the exposed and infected pregnant women are shared with the healthcare provider. Let the objective function of the wearable devices as used in Ref. [33] be denoted as

$$\Delta = \frac{A + P + t + h}{\rho} \tag{5}$$

where A is the identification of infection, P is pregnant women with different type of diseases or infections, t is the period and h is infirmaries of identification. Also, κ is the energy of the wearable devices, while δ is the working functionality of the device which is a reducing function that reduces the workload of the device. α, γ *and* φ illustrates the rate at which the biosensor of the wearable devices collect data from susceptible, exposed and infected pregnant women with wearables respectively. ξ is the rate movement of pregnant women with wearables who

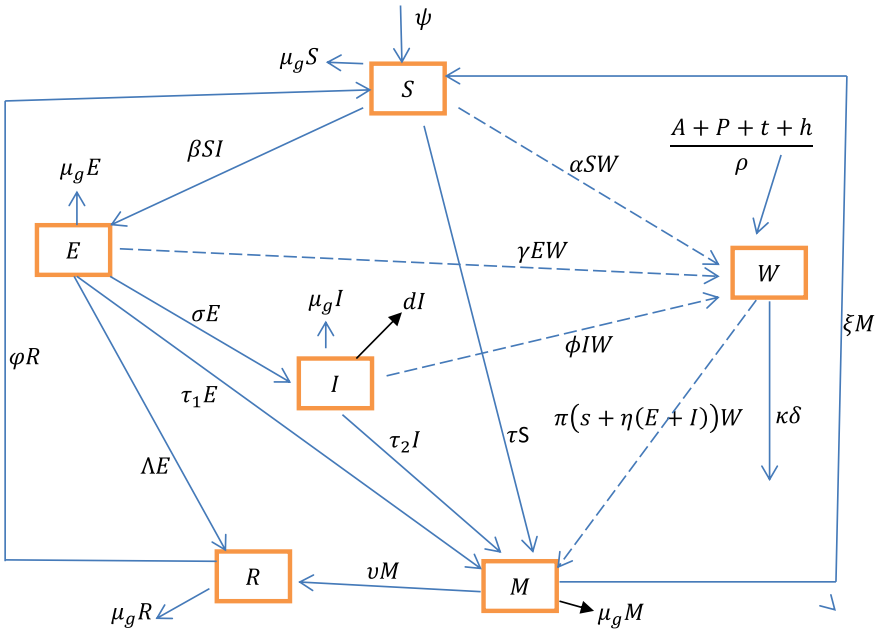

Fig. 1. Flow Diagram of Model for Monitoring Pregnant Women's Health using WHMDs.

after normal consultation with the healthcare providers return to the susceptible class. $\tau, \tau_1, and\ \tau_2$ is the rate of movement of susceptible, exposed, and infected pregnant women with wearables respectively to consultation and treatment class. φ is the rate at which the recovered pregnant women with wearables move to the susceptible class because of impaired immune function. β is the rate at which susceptible pregnant women with wearablesbecome exposed to diseases or infections. Exposed pregnant women with wearable can become infectious at the rate σ. The exposed may recover at a rate constant Λ. The susceptible pregnant women with wearables are recruited into the population at a rate constant ψ.

From the assumptions and description of the parameters and variables, the model flow diagram is shown in Fig. 1. The variables are denoted as.

$S(t)$ = Susceptible Pregnant Women with WHMDs
$E(t)$ = Exposed Pregnant Women with WHMDs
$I(t)$ = Infected Pregnant Women with WHMDs
$M(t)$ = Monitored and Treated Pregnant Women with WHMDs
$R(t)$ = Recovered Pregnant Women with WHMDs
$W(t)$ = WHMDs

The total population of pregnant patients with WHMDs at time t is given by Equ. (6)

$$N_1(t) = S(t) + E(t) + I(t) + M(t) + R(t) \tag{6}$$

The wearable healthcare device population at time t is denoted byEqu (7).

$$N_2(t) = W(t) \tag{7}$$

Therefore, we have the entire population of the proposed model at time t as

$$N(t) = N_1(t) + N_2(t) \tag{8}$$

$$N(t) = S(t) + E(t) + I(t) + M(t) + R(t) + W(t) \tag{9}$$

Therefore, the classical model is given by Equ (10).

$$\left.\begin{aligned}
\frac{dS(t)}{dt} &= \psi + \xi M + \varphi R - (\beta I + \alpha W + \tau + \mu_g)S \\
\frac{dE(t)}{dt} &= \beta IS - (\gamma W + \sigma + \Lambda + \tau_1 + \mu_g)E \\
\frac{dI(t)}{dt} &= \sigma E - (\varphi W + \tau_2 + \mu_g + d)I \\
\frac{dM(t)}{dt} &= \tau S + \tau_1 E + \tau_2 I + \lambda W - (\upsilon + \xi + \mu_g)M \\
\frac{dR(t)}{dt} &= \Lambda \mathrm{E} + \upsilon M - (\varphi + \mu_g)R \\
\frac{dW(t)}{dt} &= \Delta + (\alpha S + \gamma E + \varphi I)W - (\lambda + \kappa\delta)W
\end{aligned}\right\} \tag{10}$$

Where $\lambda = \pi(S + \eta(E + I))$ *and* $\Delta = \frac{A+P+t+h}{\rho}$.

Transformation of Equ. (10) into fractional order model under the Caputo sense yields.

$$\left.\begin{aligned}
{}^{C}_{a}D^{\varepsilon}_{0,t}S(t) &= \psi + \xi M + \varphi R - (\beta I + \alpha W + \tau + \mu_g)S \\
{}^{C}_{a}D^{\varepsilon}_{0,t}E(t) &= \beta IS - (\gamma W + \sigma + \Lambda + \tau_1 + \mu_g)E \\
{}^{C}_{a}D^{\varepsilon}_{0,t}I(t) &= \sigma E - (\varphi W + \tau_2 + \mu_g + d)I \\
{}^{C}_{a}D^{\varepsilon}_{0,t}M(t) &= \tau S + \tau_1 E + \tau_2 I + \lambda W - (\upsilon + \xi + \mu_g)M \\
{}^{C}_{a}D^{\varepsilon}_{0,t}R(t) &= \Lambda \mathrm{E} + \upsilon M - (\varphi + \mu_g)R \\
{}^{C}_{a}D^{\varepsilon}_{0,t}W(t) &= \Delta + (\alpha S + \gamma E + \varphi I)W - (\lambda + \kappa\delta)W
\end{aligned}\right\} \tag{11}$$

along with the initial value conditions $S(t) \geq 0, E(t) \geq 0, I(t) \geq 0, M(t) \geq 0, R(t) \geq 0, W(t) \geq 0$.

Hereafter, this work will make active reference to Equ (11).

3. Fractional order model design

3.1. Existence of the fractional order model and its uniqueness

In this subsection, we aim to rigorously establish the existence and uniqueness of the model utilizing the Caputo operator. This will be accomplished by directing the focus towards a real-valued, continuous function represented as $\mathscr{C}(\mathscr{Y})$,. It's noteworthy that $\mathscr{C}(\mathscr{Y})$, is situated within the framework of a Banach space on $\mathscr{Y}[0,\mathscr{J}]$ and is endowed with a norm that conforms to standard norms in functional analysis as follows.

$$\|S,E,I,M,R,W\| = \|S\| + \|E\| + \|I\| + \|M\| + \|R\| + \|W\|$$

Where $\|S\| = Sup_{t\in\mathscr{Y}}|S(t)|, \|E\| = Sup_{t\in\mathscr{Y}}|E(t)|, \|I\| = Sup_{t\in\mathscr{Y}}|I(t)|, \|M\| = Sup_{t\in\mathscr{Y}}|M(t)|, \|R\| = Sup_{t\in\mathscr{Y}}|R(t)|$ *and* $\|W\| = Sup_{t\in\mathscr{Y}}|W(t)|$.

Using the Caputo integral operator on Equ (11), we have

$$\left.\begin{aligned} S(t)-S(0) &= {}^{C}_{a}D^{\varepsilon}_{0,t}\{\psi+\xi M+\varphi R-(\beta I+\alpha W+\tau+\mu_g)S\}\\ E(t)-E(0) &= {}^{C}_{a}D^{\varepsilon}_{0,t}\{\beta IS-(\gamma W+\sigma+\Lambda+\tau_1+\mu_g)E\}\\ I(t)-I(0) &= {}^{C}_{a}D^{\varepsilon}_{0,t}\{\sigma E-(\varphi W+\tau_2+\mu_g+d)I\}\\ M(t)-M(0) &= {}^{C}_{a}D^{\varepsilon}_{0,t}\{\tau S+\tau_1 E+\tau_2 I+\lambda W-(\upsilon+\xi+\mu_g)M\}\\ R(t)-R(0) &= {}^{C}_{a}D^{\varepsilon}_{0,t}\{\Lambda\mathrm{E}+\upsilon M-(\varphi+\mu_g)R\}\\ W(t)-W(0) &= {}^{C}_{a}D^{\varepsilon}_{0,t}\{\Delta+(\alpha S+\gamma E+\varphi I)W-(\lambda+\kappa\delta)W\} \end{aligned}\right\} \quad (12)$$

We, therefore, have the model expression in system (12) referred to

$$\left.\begin{aligned} S(t)-S(0) &= V(v)\int_0^t (t-k)^{-v}U_1(v,k,S(k))dk\\ E(t)-E(0) &= V(v)\int_0^t (t-k)^{-v}U_2(v,k,E(k))dk\\ I(t)-I(0) &= V(v)\int_0^t (t-k)^{-v}U_3(v,k,I(k))dk\\ M(t)-M(0) &= V(v)\int_0^t (t-k)^{-v}U_4(v,k,M(k))dk\\ R(t)-R(0) &= V(v)\int_0^t (t-k)^{-v}U_5(v,k,R(k))dk\\ W(t)-W(0) &= V(v)\int_0^t (t-k)^{-v}U_6(v,k,W(k))dk \end{aligned}\right\} \quad (13)$$

Thus, the kernels are defined as follows.

$$\left.\begin{aligned} U_1(v,k,S(k)) &= \psi+\xi M+\varphi R-(\beta I+\alpha W+\tau+\mu_g)S\\ U_2(v,k,E(k)) &= \beta IS-(\gamma W+\sigma+\Lambda+\tau_1+\mu_g)E\\ U_3(v,k,I(k)) &= \sigma E-(\varphi W+\tau_2+\mu_g+d)I\\ U_4(v,k,M(k)) &= \tau S+\tau_1 E+\tau_2 I+\lambda W-(\upsilon+\xi+\mu_g)M\\ U_5(v,k,R(k)) &= \Lambda\mathrm{E}+\upsilon M-(\varphi+\mu_g)R\\ U_6(v,k,W(k)) &= \Delta+(\alpha S+\gamma E+\varphi I)W-(\lambda+\kappa\delta)W \end{aligned}\right\} \quad (14)$$

From (14), $U_i(i=1,2,\ldots,6)$ must ensure the validity of the Lipschitz condition by: $S(t),E(t),I(t),M(t),R(t)$ *and* $W(t)$ as upper bounds. By considering $S(t)$ *and* $\widehat{S}(t)$, we obtain

$$\|U_1(v,k,S(k)) - U_1(v,k,\widehat{S}(k))\| = \|-(\beta I+\alpha W+\tau+\mu_g)S-\widehat{S}(t)\|$$

If we assume that $\widehat{\Pi}_1 = \|-(\beta I+\alpha W+\tau+\mu_g)\|$, we therefore obtain.

$$\|U_1(v,k,S(k)) - U_1(v,k,\widehat{S}(k))\| \le \|\widehat{\Pi}_1 S(t)-\widehat{S}(t)\|$$

Thus, applying the same process to the remaining sub-equations in (14), we obtain

$$\left.\begin{aligned} \|U_2(v,k,E(k))-U_2(v,k,\widehat{E}(k))\| &\le \|\widehat{\Pi}_2 E(t)-\widehat{E}(t)\|\\ \|U_3(v,k,I(k))-U_3(v,k,\widehat{I}(k))\| &\le \|\widehat{\Pi}_3 I(t)-\widehat{I}(t)\|\\ \|U_4(v,k,M(k))-U_4(v,k,\widehat{M}(k))\| &\le \|\widehat{\Pi}_4 M(t)-\widehat{M}(t)\|\\ \|U_5(v,k,R(k))-U_5(v,k,\widehat{R}(k))\| &\le \|\widehat{\Pi}_5 R(t)-\widehat{R}(t)\|\\ \|U_6(v,k,W(k))-U_1(v,k,\widehat{W}(k))\| &\le \|\widehat{\Pi}_6 W(t)-\widehat{W}(t)\| \end{aligned}\right\} \quad (17)$$

In this form, the Lipschitz condition for the kernels is then established. Furthermore, Equ (17) can recursively be expressed as

$$\left.\begin{aligned} S(t) &= V(v)\int_0^t (t-k)^{-v}U_1(v,k,S_{n-1}(k))dk\\ E(t) &= V(v)\int_0^t (t-k)^{-v}U_2(v,k,E_{n-1}(k))dk\\ I(t) &= V(v)\int_0^t (t-k)^{-v}U_3(v,k,I_{n-1}(k))dk\\ M(t) &= V(v)\int_0^t (t-k)^{-v}U_4(v,k,M_{n-1}(k))dk\\ R(t) &= V(v)\int_0^t (t-k)^{-v}U_5(v,k,R_{n-1}(k))dk\\ W(t) &= V(v)\int_0^t (t-k)^{-v}U_6(v,k,W_{n-1}(k))dk \end{aligned}\right\} \quad (18)$$

Jointly with the initial conditions $S\ge 0, E\ge 0, I\ge 0, M\ge 0, R\ge 0, W\ge 0$, we thus get

$$\left.\begin{aligned} \mathscr{J}S_n(t) &= S(t)-S_{n-1}(t) = V(v)\int_0^t (t-k)^{-v}(U_1(v,k,S_{n-1}(k))-U_1(v,k,S_{n-2}(k)))dk\\ \mathscr{J}E_n(t) &= E(t)-E_{n-1}(t) = V(v)\int_0^t (t-k)^{-v}(U_2(v,k,E_{n-1}(k))-U_2(v,k,E_{n-2}(k)))dk\\ \mathscr{J}I_n(t) &= I(t)-I(t) = V(v)\int_0^t (t-k)^{-v}(U_3(v,k,I_{n-1}(k))-U_3(v,k,I_{n-2}(k)))dk\\ \mathscr{J}M_n(t) &= M(t)-M_{n-1}(t) = V(v)\int_0^t (t-k)^{-v}(U_4(v,k,M_{n-1}(k))-U_4(v,k,M_{n-2}(k)))dk\\ \mathscr{J}R_n(t) &= R(t)-R_{n-1}(t) = V(v)\int_0^t (t-k)^{-v}(U_5(v,k,R_{n-1}(k))-U_5(v,k,R_{n-2}(k)))dk\\ \mathscr{J}W_n(t) &= W(t)-W_{n-1}(t) = V(v)\int_0^t (t-k)^{-v}(U_6(v,k,W_{n-1}(k))-U_6(v,k,W_{n-2}(k)))dk \end{aligned}\right\} \quad (19)$$

It is relevant to think about

$$S(t)=\sum_{i=0}^{n}\mathcal{J}S_i(t),E(t)=\sum_{i=0}^{n}\mathcal{J}E_i(t),I(t)=\sum_{i=0}^{n}\mathcal{J}I_i(t),M(t)$$
$$=\sum_{i=0}^{n}\mathcal{J}M_i(t),R(t)=\sum_{i=0}^{n}\mathcal{J}R_i(t),W(t)=\sum_{i=0}^{n}\mathcal{J}W_i(t)$$

Suppose that

$$\mathcal{J}S_{n-1}(t)=S_{n-1}(t)-S_{n-2}(t),\mathcal{J}E_{n-1}(t)=E_{n-1}(t)-E_{n-2}(t),\mathcal{J}I_{n-1}(t)$$
$$=I_{n-1}(t)-I_{n-2}(t),\mathcal{J}M_{n-1}(t)$$
$$=M_{n-1}(t)-M_{n-2}(t),\mathcal{J}R_{n-1}(t)$$
$$=R_{n-1}(t)-R_{n-2}(t),\mathcal{J}W_{n-1}(t)$$
$$=W_{n-1}(t)-W_{n-2}(t)$$

and from Equ. (14) and (15), we obtain Equ (20)

$$\left.\begin{aligned}
\|\mathcal{J}S_n(t)\|&\le V(v)\varkappa_1\int_0^t(t-k)^{-v}\|\mathcal{J}S_{n-1}(k)\|dk\\
\|\mathcal{J}E_n(t)\|&\le V(v)\varkappa_2\int_0^t(t-k)^{-v}\|\mathcal{J}E_{n-1}(k)\|dk\\
\|\mathcal{J}I_n(t)\|&\le V(v)\varkappa_3\int_0^t(t-k)^{-v}\|\mathcal{J}I_{n-1}(k)\|dk\\
\|\mathcal{J}M_n(t)\|&\le V(v)\varkappa_4\int_0^t(t-k)^{-v}\|\mathcal{J}M_{n-1}(k)\|dk\\
\|\mathcal{J}R_n(t)\|&\le V(v)\varkappa_5\int_0^t(t-k)^{-v}\|\mathcal{J}R_{n-1}(k)\|dk\\
\|\mathcal{J}W_n(t)\|&\le V(v)\varkappa_6\int_0^t(t-k)^{-v}\|\mathcal{J}W_{n-1}(k)\|dk
\end{aligned}\right\}\tag{20}$$

Theorem 3.1. The governing model for monitoring the health of pregnant women with WHMDs possesses a unique solution for t ∈ [0,𝒿], if $\frac{V(v)}{V}\mathcal{J}^{v}\varkappa_i<1,i=1,2,\ldots,6$.

Proof. The boundedness and existence of (S(t), E(t), I(t), M(t), R(t), W(t)) have been established andEqu (15) and (16) are Lipschitz. Therefore, combining Equ.(20) with a recursive hypothesis, we obtainEqu (21).

$$\left.\begin{aligned}
\|\mathcal{J}S_n(t)\|&\le\|S_0(t)\|\left(\frac{V(v)}{V}\mathcal{J}^{v}\varkappa_1\right)^n\\
\|\mathcal{J}E_n(t)\|&\le\|E_0(t)\|\left(\frac{V(v)}{V}\mathcal{J}^{v}\varkappa_2\right)^n\\
\|\mathcal{J}I_n(t)\|&\le\|I_0(t)\|\left(\frac{V(v)}{V}\mathcal{J}^{v}\varkappa_3\right)^n\\
\|\mathcal{J}M_n(t)\|&\le\|M_0(t)\|\left(\frac{V(v)}{V}\mathcal{J}^{v}\varkappa_4\right)^n\\
\|\mathcal{J}R_n(t)\|&\le\|R_0(t)\|\left(\frac{V(v)}{V}\mathcal{J}^{v}\varkappa_5\right)^n\\
\|\mathcal{J}W_n(t)\|&\le\|W_0(t)\|\left(\frac{V(v)}{V}\mathcal{J}^{v}\varkappa_6\right)^n
\end{aligned}\right\}\tag{21}$$

Imposing triangular inequality for any k from Equ (21), we have

$$\|S_{n+k}(t)-S_n(t)\|\le\sum_{b=n+1}^{n+k}d_1^i=\frac{d_1^{n+1}-d_1^{n+k+1}}{1-d_1}$$
$$\|E_{n+k}(t)-E_n(t)\|\le\sum_{b=n+1}^{n+k}d_2^i=\frac{d_2^{n+1}-d_2^{n+k+1}}{1-d_2}$$
$$\|I_{n+k}(t)-I_n(t)\|\le\sum_{b=n+1}^{n+k}d_3^i=\frac{d_3^{n+1}-d_3^{n+k+1}}{1-d_3}$$
$$\|M_{n+k}(t)-M_n(t)\|\le\sum_{b=n+1}^{n+k}d_4^i=\frac{d_4^{n+1}-d_4^{n+k+1}}{1-d_4}$$
$$\|R_{n+k}(t)-R_n(t)\|\le\sum_{b=n+1}^{n+k}d_5^i=\frac{d_5^{n+1}-d_5^{n+k+1}}{1-d_5}$$
$$\|W_{n+k}(t)-W_n(t)\|\le\sum_{b=n+1}^{n+k}d_6^i=\frac{d_6^{n+1}-d_6^{n+k+1}}{1-d_6}\tag{22}$$

It can be deduced hypothetically that $\mathscr{k}_i=\frac{V(v)}{V}\mathcal{J}^{v}\varkappa_i<1$. Thus, $S_n, E_n, I_n, M_n, R_n, W_n$ are known as the Cauchy sequence in $\mathscr{C}(\mathscr{Y})$ and are uniformly convergent. Applying the proposition on the limit in system (15) as $n\to\infty$ shows that Equ (11) is unique.

3.2. Invariant region

The fractional order model Equ (11) is analyzed in a feasible region, such that the model is considered in two-part, $N_1(t)=S(t)+E(t)+I(t)+M(t)+R(t)$ for the total population of pregnant women with wearable healthcare devices and $N_2(t)=W(t)$ for the wearable healthcare devices population.

Theorem 3.2. *The region* $\Omega=\Omega_1\times\Omega_2$ *where* $\Omega_1=\left\{(S(t),E(t),I(t),M(t),R(t))\in\mathbb{R}_+^5:0\le N_1\le\frac{\psi}{\mu_g}\right\}$ *and* $\Omega_2=\left\{W(t)\in\mathbb{R}_+^1:0\le N_2\le\frac{\Delta}{\kappa\delta}\right\}$ *is positively invariant.*

Proof. *The total population of pregnant patients with WHMD is considered such that in the absence of any disease during pregnancy, we have*

$${}_a^C D_{0,t}^{\varepsilon}N(t)=\psi-(S+E+I+M+R)\mu_g$$
$$=\psi-\mu_g\mathrm{N}_1\tag{23}$$
$$\frac{d}{dt}(\mathrm{N}_1e^{\mu_g t^{\varepsilon}})=\psi\tag{24}$$
$$\mathrm{N}_1(t)=\frac{\psi}{\mu_g}(1-e^{-\mu_g t^{\varepsilon}})\tag{25}$$

Similarly, for the WHMDs we then have

$$\mathrm{N}_2(t)=\frac{\Delta}{\kappa\delta}(1-e^{\kappa\delta t^{\varepsilon}})\tag{26}$$

As $t\to\infty$ in systems (25) and (20), the total population of pregnant women with WHMDs and the wearable devices respectively starts and in the feasible regions.

$$\left.\begin{aligned}\Omega_1=\left\{(S(t),E(t),I(t),M(t),R(t))\in\mathbb{R}_+^5:0\le N_1\le\frac{\psi}{\mu_g}\right\}\\ \text{and }\Omega_2=\left\{W(t)\in\mathbb{R}_+^1:0\le N_2\le\frac{\Delta}{\kappa\delta}\right\}\end{aligned}\right\}\tag{27}$$

Therefore, Equ (27) shows that $S(t), E(t), I(t), M(t), R(t)$ *and* $W(t)$ are bounded for all $t>0$ and are not capable of leaving Ω which implies that the fractional order model Equ (11) is positively invariant.

Theorem 3.3. The fractional order model solutions of Equ (15) and initial value conditions S(t) ≥ 0, E(t) ≥ 0, I(t) ≥ 0, M(t) ≥ 0, R(t) ≥ 0, W(t) ≥ 0 are non-negative for all t > 0.

Proof. From the first sub-equation of the model system (11) we have

$$ {}_a^C D_{0,t}^{\varepsilon} S(t) = \psi + \xi M + \varphi R - \left(\beta I + \alpha W + \tau + \mu_g\right) S \geq -\left(\beta I + \alpha W + \tau + \mu_g\right) S \tag{28} $$

$$ {}_a^C D_{0,t}^{\varepsilon} S(t) \geq -\left(\beta I + \alpha W + \tau + \mu_g\right) dt \tag{29} $$

$$ \int {}_a^C D_{0,t}^{\varepsilon} S(t) \geq -\int \left(\beta I + \alpha W + \tau + \mu_g\right) dt \tag{30} $$

Equ (30) yields

$$ {}_a^C D_{0,t}^{\varepsilon} S(t) \geq S(0) e^{\left(\beta I + \alpha W + \tau + \mu_g\right) t} > 0 \tag{31} $$

Applying the same computation process to the remaining sub-equations of system (11) gives

$$ \left.\begin{aligned} {}_a^C D_{0,t}^{\varepsilon} E(t) &\geq E(0) e^{\left(\gamma W + \sigma + \Lambda + \tau_1 + \mu_g\right) t} > 0 \\ {}_a^C D_{0,t}^{\varepsilon} I(t) &\geq I(0) e^{\left(\varphi W + \tau_2 + \mu_g + d\right) t} > 0 \\ {}_a^C D_{0,t}^{\varepsilon} M(t) &\geq M(0) e^{\left(\upsilon + \xi + \mu_g\right) t} > 0 \\ {}_a^C D_{0,t}^{\varepsilon} R(t) &\geq R(0) e^{\left(\varphi + \mu_g\right) t} > 0 \\ {}_a^C D_{0,t}^{\varepsilon} W(t) &\geq W(0) e^{(\lambda + \kappa\delta) t} > 0 \end{aligned}\right\} \tag{32} $$

Thus, the solutions of Equ (11) are positive.

3.3. Equilibrium solution of the model

In this section, we observe that Equ (11) has two equilibria namely, disease-free equilibrium and disease–present equilibrium among pregnant patients with WHMD solution. To obtain the equilibrium solutions, we equate the left-hand side of Equ (11) to zero and we have the disease-free equilibrium solution for pregnant patients with device given byEqu (33)

$$ E_q^0 = (S, E, I, M, R, W) = \left(\frac{\psi}{\mu_g}, 0, 0, 0, 0, \frac{\Delta}{\kappa\delta}\right) \tag{33} $$

Similarly, the disease–present equilibrium solution for pregnant patients with wearable healthcare devices is given as

$$ E_q^* = (S^*, E^*, I^*, M^*, R^*, W^*) = $$

$$ \left.\begin{aligned} S^* &= \frac{\psi + \xi M^* + \varphi R^*}{\beta I^* + \alpha W^* + \tau + \mu_g} \\ E^* &= \frac{\beta S^* I^*}{\gamma W^* + \sigma + \Lambda + \tau_1 + \mu_g} \\ I^* &= \frac{\sigma E^*}{\varphi W^* + \tau_2 + \mu_g + d} \\ M^* &= \frac{\tau_2 I^* + \lambda W^*}{\upsilon + \xi + \mu_g} \\ R^* &= \frac{\Lambda E^* + \upsilon M^*}{\varphi + \mu_g} \\ W^* &= \frac{\Delta}{\lambda + \kappa\delta - (\alpha S^* + \gamma E^* + \varphi I^*)} \end{aligned}\right\} \tag{34} $$

3.4. Basic reproduction number R_W computation

The basic reproduction number R_W of diseases among pregnant patients with WHMD denotes the average rate at which new health cases among these categories of patients occur in the population. The next generation matrix method FV^{-1} [32,34,35] is engaged in computing R_W of model system (11) and is given byEqu (35).

$$ R_W = \frac{\beta\psi}{\mu_g\left(\gamma W + \sigma + \Lambda + \tau_1 + \mu_g\right)} \tag{35} $$

The threshold in (33) implies that, when $R_W < 1$, wearable healthcare monitoring devices were able to collect and transmit data in real-time to enable healthcare providers or qualified doctorsto direct pregnant patient on the necessary specific measures to improve their health and control the disease in the population.

3.5. Sensitivity analysis of R_W in the presence of WHMD

To control diseases among pregnant patients, WHMD must be able to track pregnant patients health data, (i.e., collect personal health data of pregnant patients and transfer same to cloud-based healthcare professionals/doctors in real-time). Such expert systems will help doctors better understand their instant health state and provide seamless interventions. From the data aggregated, healthcare providers can identify health challenged patients quickly and offer quick solutions. This will help in the control of new cases complications among pregnant patients in the population such that $R_W < 1$.

We, therefore, find the rate of change of R_W with respect to γW from the normalized sensitivity index given by

$$ Z_{\gamma W}^{R_W} = \frac{\partial R_W}{\partial \gamma W} \cdot \frac{R_W}{\gamma W} = -\frac{(\beta\psi)^2}{\gamma W \left(\mu_g\right)^2 \left(\gamma W + \sigma + \Lambda + \tau_1 + \mu_g\right)^3} \tag{36} $$

We observe that the sensitivity index $Z(\gamma W)$ is negative and this indicates that the rateat which new cases of disease among pregnant patients with WHMD (R_W) decreases in the presence of wearable devices.

4. Fractional optimal control problems (FOCPs)

The control variables are strategies that detect data (u_1) of the susceptible, exposed, and infected pregnant patients with health imbalances (diseases) using WHMD, the effective data transmission rate (u_2) and reduction of these health imbalances (diseases) among pregnant patients via treatment (u_3) from healthcare experts in real-time. In the model, WHMD detects pregnant patients with health problems (u_1) is incorporated in the compartments *S*,*E and I*. Furthermore, effective data transmission (u_2) and treatment (u_3) control functions are employed on compartments *S*, *E and I*. This process aims to reduce the number of exposed and infected pregnant patients by moving them to the recovered category. By considering the state Equ. (11) in $\mathbb{R}_+^6$, we let $\mathbb{W} = \{u_1(t), u_2(t), u_3(t)$ *are Lebsegue measurable*, $0 \leq u_1(t), u_2(t), u_3(t) \leq 1 \; \forall \; t \in [0, t_f]\}$ be the admissible control set. The objective functionis defined as follows:

$$ \mathscr{J}(u_1, u_2, u_3) = \int_0^{t_f} \left(AS(t) + Bu_1^2(t) + Cu_2^2(t) + Du_3^2(t)\right) dt \tag{37} $$

Where *A* is the weight constant of susceptible pregnant patient with WHMD. Also, *B and C* are respectively the weight constant for detection and transmission of health imbalances among pregnant patient, while *D* isthe weight constant for treatment by healthcare providers or qualified doctors. In order words, we aim to minimize the following objective function in Equ (36).

$$ \mathscr{J}(u_1, u_2, u_3) = \int_0^{t_f} \zeta(S, E, I, M, R, W, t) dt \tag{38} $$

Subject to the constraints

$$ {}_a^C D_{0,t}^{\varepsilon} S(t) = \ell_1, {}_a^C D_{0,t}^{\varepsilon} E(t) = \ell_2, {}_a^C D_{0,t}^{\varepsilon} I(t) = \ell_3, {}_a^C D_{0,t}^{\varepsilon} M(t) = \ell_4, {}_a^C D_{0,t}^{\varepsilon} R(t) = \ell_5, {}_a^C D_{0,t}^{\varepsilon} W(t) = \ell_6 $$

Where $\ell_i = \ell(S, E, I, M, R, W, t), i = 1, 2, \ldots, 6$, with the following initial conditions $S(0) = S_0, E(0) = E_0, I(0) = I_0, M(0) = M_0, R(0) = R_0, W(0) =$

W_0.

We define the modified objective function using Sweilam and Al-Mekhlafi [36],

$$\widehat{\mathscr{J}}\int_0^{t_f}\left[H_a(S,E,I,M,R,W,u_1,u_2,u_3,t)-\sum_{i=1}^{6}\lambda_i\mathscr{L}_i(S,E,I,M,R,W,u_1,u_2,u_3,t)\right]dt \tag{39}$$

Therefore, the Hamiltanain is given as follows

$$H_a(S,E,I,M,R,W,u_1,u_2,u_3,\lambda_i,t)=\zeta(S,E,I,M,R,W,u_1,u_2,u_3,t)+\lambda_i\mathscr{L}_i(S,E,I,M,R,W,u_1,u_2,u_3,t) \tag{40}$$

From Equ. (37) and (38), we have that the necessary conditions for fractional optimal control Problems [37–40] are

$$\begin{aligned}{}_t^C D_{t_f}^{\varepsilon}\lambda_S &= -\frac{\partial H_a}{\partial S},\ {}_t^C D_{t_f}^{\varepsilon}\lambda_E=-\frac{\partial H_a}{\partial E},\ {}_t^C D_{t_f}^{\varepsilon}\lambda_I=-\frac{\partial H_a}{\partial I},\ {}_t^C D_{t_f}^{\varepsilon}\lambda_M=-\frac{\partial H_a}{\partial M},\ {}_t^C D_{t_f}^{\varepsilon}\lambda_R\\ &= -\frac{\partial H_a}{\partial R},\ {}_t^C D_{t_f}^{\varepsilon}\lambda_W=-\frac{\partial H_a}{\partial W}\end{aligned} \tag{41}$$

$$\text{Moreover},\frac{\partial H_a}{\partial u_j}=0 \tag{42}$$

$$\begin{aligned}{}_0^C D_t^{\varepsilon}S &= -\frac{\partial H_a}{\partial \lambda_S},\ {}_0^C D_t^{\varepsilon}E=-\frac{\partial H_a}{\partial \lambda_E},\ {}_0^C D_t^{\varepsilon}I=-\frac{\partial H_a}{\partial \lambda_I},\ {}_0^C D_t^{\varepsilon}M=-\frac{\partial H_a}{\partial \lambda_M},\ {}_0^C D_t^{\varepsilon}R\\ &= -\frac{\partial H_a}{\partial \lambda_R},\ {}_0^C D_t^{\varepsilon}W=-\frac{\partial H_a}{\partial \lambda_W}\end{aligned} \tag{43}$$

$$\text{Also},\lambda_i(t_f)=0 \tag{44}$$

Where $\lambda_i, i = S,E,I,M,R,W$, are the Lagrange multipliers.

Theorem 4.1. *If u_1^*,u_2^*,u_3^* be the optimal controls with corresponding states $S^{**},E^{**},I^{**},M^{**},R^{**}$ and W^{**}, then there exist adjoint variables $\lambda_i^*, i = S,E,I,M,R,W$ that meets the following requirements in Equ*(44).

(i) Adjoint Computations

With the transversality conditions at the time t_f such that

$$\lambda_i(t_f)=0, i=S,E,I,M,R,W \tag{45}$$

The optimality conditions are given as

$$H_a(S,E,I,M,R,W,u_1,u_2,u_3,\lambda_i)=\underset{0\le u_1,u_2,u_3\le 1}{\text{Min}}H_a(S,E,I,M,R,W,u_1,u_2,u_3,\lambda_i) \tag{46}$$

Additionally, the control functions u_1^*,u_2^*,u_3^* are given as

$$\left.\begin{aligned}u_1^* &= \frac{W^{**}\left[S^{**}\left(\lambda_S^*-\lambda_W^*\right)+E^{**}\left(\lambda_E^*-\lambda_W^*\right)+I^{**}\left(\lambda_I^*-\lambda_W^*\right)\right]}{2B}\\ u_2^* &= \frac{\left(S^{**}+\eta(E^{**}+I^{**})\right)W^{**}\left(\lambda_W^*-\lambda_M^*\right)}{2C}\\ u_3^* &= \frac{S^{**}\left(\lambda_S^*-\lambda_M^*\right)+E^{**}\left(\lambda_E^*-\lambda_M^*\right)+I^{**}\left(\lambda_I^*-\lambda_M^*\right)}{2D}\end{aligned}\right\} \tag{47}$$

$$\left.\begin{aligned}u_1^* &= \min\left\{1,\max\left\{0,\frac{W^{**}\left[S^{**}\left(\lambda_S^*-\lambda_W^*\right)+E^{**}\left(\lambda_E^*-\lambda_W^*\right)+I^{**}\left(\lambda_I^*-\lambda_W^*\right)\right]}{2B}\right\}\right\}\\ u_2^* &= \min\left\{1,\max\left\{0,\frac{\left(S^{**}+\eta(E^{**}+I^{**})\right)W^{**}\left(\lambda_W^*-\lambda_M^*\right)}{2C}\right\}\right\}\\ u_3^* &= \min\left\{1,\max\left\{0,\frac{S^{**}\left(\lambda_S^*-\lambda_M^*\right)+E^{**}\left(\lambda_E^*-\lambda_M^*\right)+I^{**}\left(\lambda_I^*-\lambda_M^*\right)}{2D}\right\}\right\}\end{aligned}\right\} \tag{48}$$

Proof. We can claim Equ(44) using the conditions in system (41) where the Hamiltonian H_a^* is given by

$$\begin{aligned}H_a^* = A &+ Bu_1^{*2}+Cu_2^{*2}+Du_3^{*2}+\lambda_{Sa}^{*C}D_{0,t}^{\varepsilon}S^{**}+\lambda_{Ea}^{*C}D_{0,t}^{\varepsilon}E^{**}+\lambda_{Ia}^{*C}D_{0,t}^{\varepsilon}I^{**}\\ &+\lambda_{Ma}^{*C}D_{0,t}^{\varepsilon}M^{**}+\lambda_{Ra}^{*C}D_{0,t}^{\varepsilon}R^{**}+\lambda_{Wa}^{*C}D_{0,t}^{\varepsilon}W^{**}\end{aligned} \tag{49}$$

Furthermore, $\lambda_i(t_f)=0, i=S,E,I,M,R,W$ *holds*. The optimality conditions (48) can be claimed from the maximization conditions (46). Substituting u_1^*,u_2^*,u_3^* in Equ (11), we have

$$\left.\begin{aligned}{}_a^C D_{0,t}^{\varepsilon}S^{**} &= \psi+\xi M^{**}+\varphi R^{**}-\left(\beta I^{**}+\alpha W^{**}+\tau+\mu_g\right)S^{**}\\ {}_a^C D_{0,t}^{\varepsilon}E^{**} &= \beta I^{**}S^{**}-\left(\gamma W^{**}+\sigma+\Lambda+\tau_1+\mu_g\right)E^{**}\\ {}_a^C D_{0,t}^{\varepsilon}I^{**} &= \sigma E^{**}-\left(\varphi W^{**}+\tau_2+\mu_g+d\right)I^{**}\\ {}_a^C D_{0,t}^{\varepsilon}M^{**} &= \tau S^{**}+\tau_1E^{**}+\tau_2I^{**}+\pi(S^{**}+\eta(E^{**}+I^{**}))W^{**}-\left(\upsilon+\xi+\mu_g\right)M^{**}\\ {}_a^C D_{0,t}^{\varepsilon}R^{**} &= \Lambda E^{**}+\upsilon M^{**}-\left(\varphi+\mu_g\right)R^{**}\\ {}_a^C D_{0,t}^{\varepsilon}W^{**} &= \Delta+(\alpha S^{**}+\gamma E^{**}+\varphi I^{**})W^{**}-(\pi(S^{**}+\eta(E^{**}+I^{**}))+\kappa\delta)W^{**}\end{aligned}\right\} \tag{50}$$

4.1. Existence of the optimal control pair

The existence of the optimal control pair of the state system (50) can be directly obtained using the results in Refs. [41,42]; thus, we use the following theorem:

Theorem 4.1. *There exists an optimal control pair $(u_1^*,u_2^*,u_3^*)\in\mathbb{W}$ such that.*

$$\mathscr{J}\left(u_1^*,u_2^*,u_3^*\right)=\min_{(u_1,u_2,u_2)\in\mathbb{W}}\mathscr{J}(u_1,u_2,u_2)$$

Proof. We use the result in Ref. [42] to present the existence of optimal control by noting that the control and state variables are non-negative values. The necessary convexity of the objective functional in u_1,u_2,u_2 are satisfied in this minimizing problem and, the set of all the control variables $(u_1,u_2,u_2)\in\mathbb{W}$ is also convex and closed. The boundedness of the optimal system determines the compactness needed for the existence of the optimal control. Furthermore, the integrand in the objective functional Equ (35) $AS+Bu_1^2+Cu_2^2+u_3^2$, is convex on the control set $\mathbb{W}$. More so, we can claim that there exist a constant $\Phi>1$ and numbers L_1, L_2 such that

$$\mathscr{J}(u_1,u_2,u_2)\ge L_1\left(u_1^2+u_2^2+u_3^2\right)^{\Phi/2}-L_2$$

This completes the existence of an optimal control since the state variables are bounded.

5. Numerical technique

In this section, we used the modified form of the numerical scheme of the differential transform method (i.e., FMSDTM) to obtain the approximate solution of the fractional order model Equ (11). By considering a system of fractional ordinary differential equations in Equ (51)

$$\left.\begin{aligned}{}_a^C D_{0,t_1}^{\varepsilon}y_1(t) &= f_1(t,y_1,y_2,\ldots,y_n)\\ {}_a^C D_{0,t_2}^{\varepsilon}y_2(t) &= f_2(t,y_1,y_2,\ldots,y_n)\\ &\vdots\\ {}_a^C D_{0,t_n}^{\varepsilon}y_n(t) &= f_n(t,y_1,y_2,\ldots,y_n)\end{aligned}\right\} \tag{51}$$

Along with the initial value conditions $y_i(0)=k_i, i=1,2,\ldots,n$, where ${}_a^C D_{0,t}^{\varepsilon}$ is a Caputo derivative of order $0<\varepsilon_i\le 1$ *for* $i=1,2,\ldots,n$. The

interval $[t_0, t_f]$ is where we determine the solution of Equ (51). The $k+h$ order approximate solution of Equ (51) is given by the finite series of the form Equ (52)

$$y_i(t) = \sum_{i=0}^{k} y_i(k)(t-t_0)^{k\varepsilon_i}, t\epsilon\left[t_0, t_f\right] \tag{52}$$

Having that $y_i(k)$ satisfies the recurrence relation;

$$\frac{\Gamma((k+1)\varepsilon_i+1)}{\Gamma(k\varepsilon_i+1)} Y_i(k+1) = F_i(k, Y_1, Y_2, \ldots, Y_n) \tag{53}$$

We have that $Y_i(0) = a_i$ *and* $F_i(k, Y_1, Y_2, \ldots, Y_n)$ are the initial conditions and differential transforms of functions $f_i(t,y_1,y_2,\ldots,y_n)$ *for* $i = 1,2,\ldots,n$. Assuming that the interval $[t_0, t_f]$ is partitioned into $\mathscr{G}$ subintervals $[t_{\mathscr{g}-1}, t_{\mathscr{g}}]$, $\mathscr{G} = 1, 2, \ldots, \mathscr{P}$ of equal step size $h = (t_f - t_0)/\mathscr{G}$ by the use of the nodes $t_{\mathscr{g}} = t_0 + \mathscr{g}h$. We apply the differential transform method to carry out the numerical implementation of Equ (54) and obtain

where $S(k), E(k), I(k), M(k), R(k)$ *and* $W(k)$ with initial conditions $S \geq 0$, $E \geq 0, I \geq 0, M \geq 0, R \geq 0$ *and* $W \geq 0$ are the differential transforms of $S(t), E(t), I(t), M(t), R(t)$ *and* $W(t)$ respectively. With regard to the differential inverse transform series solution for Equ (55) as

$$\begin{aligned} S(t) = \sum_{n=0}^{N} S(n)t^{\varepsilon_{1,n}}, E(t) = \sum_{n=0}^{N} E(n)t^{\varepsilon_{2,n}}, I(t) = \sum_{n=0}^{N} I(n)t^{\varepsilon_{3,n}}, M(t) \\ = \sum_{n=0}^{N} M(n)t^{\varepsilon_{4,n}}, R(t) = \sum_{n=0}^{N} R(n)t^{\varepsilon_{5,n}}, W(t) \\ = \sum_{n=0}^{N} W(n)t^{\varepsilon_{6,n}} \end{aligned} \tag{55}$$

At this juncture, we apply the FMSDTM and have Equs (40) and (41) given as Equ. (56).

$$\left.\begin{aligned} S(k+1) &= \frac{\Gamma(k\varepsilon_i+1)}{\Gamma((k+1)\varepsilon_i+1)}\left((\psi + \xi M(k-l) + \varphi R(k-l)) - \left(\beta I(k-l) + \alpha W(k-l) + \tau + \mu_g\right)S(k)\right) \\ E(k+1) &= \frac{\Gamma(k\varepsilon_i+1)}{\Gamma((k+1)\varepsilon_i+1)}\left((\beta I(k-l)S(k-l)) - \left(\gamma W(k-l) + \sigma + \Lambda + \tau_1 + \mu_g\right)E(k)\right) \\ I(k+1) &= \frac{\Gamma(k\varepsilon_i+1)}{\Gamma((k+1)\varepsilon_i+1)}\left(\sigma E(k-l) - \left(\varphi W(k-l) + \tau_2 + \mu_g + d\right)I(k)\right) \\ M(k+1) &= \frac{\Gamma(k\varepsilon_i+1)}{\Gamma((k+1)\varepsilon_i+1)}\left(\begin{pmatrix} \tau S(k-l) + \tau_1 E(k-l) + \tau_2 I(k-l) \\ \\ +\pi(S(k-l) + \eta(E(k-l) + I(k-l))W(k-l)) \end{pmatrix} - \left(\upsilon + \xi + \mu_g\right)M(k)\right) \\ R(k+1) &= \frac{\Gamma(k\varepsilon_i+1)}{\Gamma((k+1)\varepsilon_i+1)}\left(\Lambda \mathrm{E(k-1)} + \upsilon M(k-l) - \left(\varphi + \mu_g\right)R(k)\right) \\ W(k+1) &= \frac{\Gamma(k\varepsilon_i+1)}{\Gamma((k+1)\varepsilon_i+1)}\begin{pmatrix} \Delta + (\alpha S(k-l) + \gamma E(k-l) + \varphi I(k-l))W(k) \\ -(\pi(S(k-l) + \eta(E(k-l) + I(k-l))) + \kappa\delta)W(k) \end{pmatrix} \end{aligned}\right\} \tag{54}$$

$$\left.\begin{aligned} s(t) &= \sum_{n=0}^{k} S_1(n)t^{\varepsilon_{1,n}}, t \in [0,t_1], \sum_{n=0}^{k} S_2(n)(t-t_1)^{\varepsilon_{1,n}}, t \in [t_1,t_2], \ldots, \sum_{n=0}^{k} S_{\mathscr{g}}(n)\left(t-t_{\mathscr{g}-1}\right)^{\varepsilon_{1,n}}, t \in \left[t_{\mathscr{g}-1}, t_{\mathscr{g}}\right] \\ e(t) &= \sum_{n=0}^{k} E_1(n)t^{\varepsilon_{1,n}}, t \in [0,t_1], \sum_{n=0}^{k} E_2(n)(t-t_1)^{\varepsilon_{1,n}}, t \in [t_1,t_2], \ldots, \sum_{n=0}^{k} E_{\mathscr{g}}(n)\left(t-t_{\mathscr{g}-1}\right)^{\varepsilon_{1,n}}, t \in \left[t_{\mathscr{g}-1}, t_{\mathscr{g}}\right] \\ i(t) &= \sum_{n=0}^{k} I_1(n)t^{\varepsilon_{1,n}}, t \in [0,t_1], \sum_{n=0}^{k} I_2(n)(t-t_1)^{\varepsilon_{1,n}}, t \in [t_1,t_2], \ldots, \sum_{n=0}^{k} I_{\mathscr{g}}(n)\left(t-t_{\mathscr{g}-1}\right)^{\varepsilon_{1,n}}, t \in \left[t_{\mathscr{g}-1}, t_{\mathscr{g}}\right] \\ m(t) &= \sum_{n=0}^{k} M_1(n)t^{\varepsilon_{1,n}}, t \in [0,t_1], \sum_{n=0}^{k} M_2(n)(t-t_1)^{\varepsilon_{1,n}}, t \in [t_1,t_2], \ldots, \sum_{n=0}^{k} M_{\mathscr{g}}(n)\left(t-t_{\mathscr{g}-1}\right)^{\varepsilon_{1,n}}, t \in \left[t_{\mathscr{g}-1}, t_{\mathscr{g}}\right] \\ r(t) &= \sum_{n=0}^{k} R_1(n)t^{\varepsilon_{1,n}}, t \in [0,t_1], \sum_{n=0}^{k} R_2(n)(t-t_1)^{\varepsilon_{1,n}}, t \in [t_1,t_2], \ldots, \sum_{n=0}^{k} R_{\mathscr{g}}(n)\left(t-t_{\mathscr{g}-1}\right)^{\varepsilon_{1,n}}, t \in \left[t_{\mathscr{g}-1}, t_{\mathscr{g}}\right] \\ w(t) &= \sum_{n=0}^{k} W_1(n)t^{\varepsilon_{1,n}}, t \in [0,t_1], \sum_{n=0}^{k} W_2(n)(t-t_1)^{\varepsilon_{1,n}}, t \in [t_1,t_2], \ldots, \sum_{n=0}^{k} W_{\mathscr{g}}(n)\left(t-t_{\mathscr{g}-1}\right)^{\varepsilon_{1,n}}, t \in \left[t_{\mathscr{g}-1}, t_{\mathscr{g}}\right] \end{aligned}\right\} \tag{56}$$

Here, $S_i(n), E_i(n), I_i(n), M_i(n), R_i(n)$ *and* $W_i(n)$ must satisfy the recurrence relation given as

$$\left.\begin{aligned}
S_i(k+1) &= \frac{\Gamma(k\varepsilon_i+1)}{\Gamma((k+1)\varepsilon_i+1)}\left((\psi+\xi M_i(k-l)+\varphi R_i(k-l))-\left(\beta I_i(k-l)+\alpha W_i(k-l)+\tau+\mu_g\right)S_i(k)\right)\\
hE_i(k+1) &= \frac{\Gamma(k\varepsilon_i+1)}{\Gamma((k+1)\varepsilon_i+1)}\left((\beta I_i(k-l)S_i(k-l))-\left(\gamma W_i(k-l)+\sigma+\Lambda+\tau_1+\mu_g\right)E_i(k)\right)\\
I_i(k+1) &= \frac{\Gamma(k\varepsilon_i+1)}{\Gamma((k+1)\varepsilon_i+1)}\left(\sigma E_i(k-l)-\left(\varphi W_i(k-l)+\tau_2+\mu_g+d\right)I_i(k)\right)\\
M_i(k+1) &= \frac{\Gamma(k\varepsilon_i+1)}{\Gamma((k+1)\varepsilon_i+1)}\begin{pmatrix}\tau S_i(k-l)+\tau_1 E_i(k-l)+\tau_2 I_i(k-l)\\ \left(\begin{matrix}\\ +\pi(S_i(k-l)+\eta(E_i(k-l)+I_i(k-l))W_i(k-l))\end{matrix}\right)\\ -\left(\upsilon+\xi+\mu_g\right)M_i(k)\end{pmatrix}\\
R_i(k+1) &= \frac{\Gamma(k\varepsilon_i+1)}{\Gamma((k+1)\varepsilon_i+1)}\left(\Lambda E_i(\mathrm{k}-1)+\upsilon M_i(k-l)-\left(\varphi+\mu_g\right)R_i(k)\right)\\
W_i(k+1) &= \frac{\Gamma(k\varepsilon_i+1)}{\Gamma((k+1)\varepsilon_i+1)}\begin{pmatrix}\Delta+(\alpha S_i(k-l)+\gamma E_i(k-l)+\varphi I_i(k-l))W_i(k)\\ -(\pi(S_i(k-l)+\eta(E_i(k-l)+I_i(k-l)))+\kappa\delta)W_i(k)\end{pmatrix}
\end{aligned}\right\} \quad (57)$$

Having that

$$\begin{aligned}
S_i(t) &= s_i(t_{i-1}) = s_{i-1}(t_{i-1}), E_i(t) = e_i(t_{i-1}) = e_{i-1}(t_{i-1}), I_i(t) = i_i(t_{i-1})\\
&= i_{i-1}(t_{i-1}), M_i(t) = m_i(t_{i-1}) = m_{i-1}(t_{i-1}), R_i(t) = r_i(t_{i-1})\\
&= r_{i-1}(t_{i-1}) \textit{ and } W_i(t) = w_i(t_{i-1}) = w_{i-1}(t_{i-1}).
\end{aligned}$$

6. Numerical simulation

In this section, results obtained are presented first by numerically solving the fractional order model Equ. (11) using the FMSDTM scheme for the model. MATLAB R2019 (9.6.0.1072779) with license number 968398 is used for this purpose. The value of the basic reproduction number in the presence of a WHMD is given as $R_W = 0.43282325$. The effectiveness of wearable telemedicine and the optimal control strategies on the transmission dynamics of infection in pregnant patients was explored by simulating the control-related parameters of the model system (6) over the time interval [0, 270]. We considered strategies that detect the following data: susceptible, exposed, and infected pregnant patients with health issues using WHMD. Also captured are the effective data transmission rate, and reduction of these health complications among pregnant patients via decision experts' agents in real-time. We simulated the proposed model system (11) using the initial conditions $S(0) = 720, E(0) = 610, I(0) = 30, M(0) = 105, R(0) = 145, W(0) = 343$. The parameter values used for model simulation were given in Table 2 showing the numerical values for vitals signals and disease control during pregnancy with wearable devices. The existing GDPR and the act of legislation are assumed in this study [60].

The behavior of the basic reproduction number of the model is shown in Fig. 2. It was observed that in the presence of WHMD, health imbalances during pregnancy are effectively controlled because infected individuals n the average will infect less than one other person. This is because, with WHMDs, the average rate of new cases of disease among pregnant patients in the population decreased. This is as a result of effective detection and transmission of data relating to the health of pregnant patients for necessary healthcare provider analytics. The results show convergence to the health imbalance-free equilibrium during pregnancy, that is, $R_W < 1$.

Fig. 3 illustrates a persistent oscillation in the populations of susceptible pregnant patients and those with wearable devices throughout the pregnancy period. The dynamic interaction between population growth and the accurate detection and transmission of health-related data plays a pivotal role in influencing the susceptibility of pregnant patients. This reciprocal relationship generates the continuous oscillation observed in both compartments. This phenomenon is further elucidated in Fig. 4. During the initial trimester, there is a noteworthy increase in both the treated and recovered populations before reaching a state of equilibrium. Subsequently, from the second to the third trimester, these populations exhibit sustained oscillations, indicating a stabilized management of health disparities among pregnant patients facilitated by the used of WHMDs.

Conversely, the populations of exposed and infected individuals remain relatively stable during the first month of the first trimester. This stability is momentarily disrupted by a slight upsurge in the second and third months of the first trimester, followed by a consistent oscillation at diminished levels during the subsequent trimesters. This pattern underscores the role of enhanced usage, precise detection, and seamless transmission of health data from pregnant patients, enabling timely consultations and treatments from healthcare experts. Ultimately, this approach leads to a reduction in the susceptible pregnant patient's population.

Table 2
Optimal Parameter values for wearable telemedicine device.

Parameters	Values	References Sources
ψ	576.9231	[22]
ξ	0.002	optimal
φ	0.05 – 0.14	optimal
$\alpha, \gamma, \varnothing$	0.045 – 0.45	optimal
η	0.08	optimal
τ, τ_1, τ_2	0.028 – 0.28	optimal
β	0.06 – 0.06	[43]
μ_g	0.02	optimal
ρ	32	[33]
d	0.426	[44]
σ	0.459	[43]
Λ	0.4	optimal
π	0.8	optimal
υ	0.1109289	optimal
κ	5	[33]
Λ	420	[33]
h	0.95	[33]
P	1.3	[33]
δ	0.55	[33]
t	270	optimal

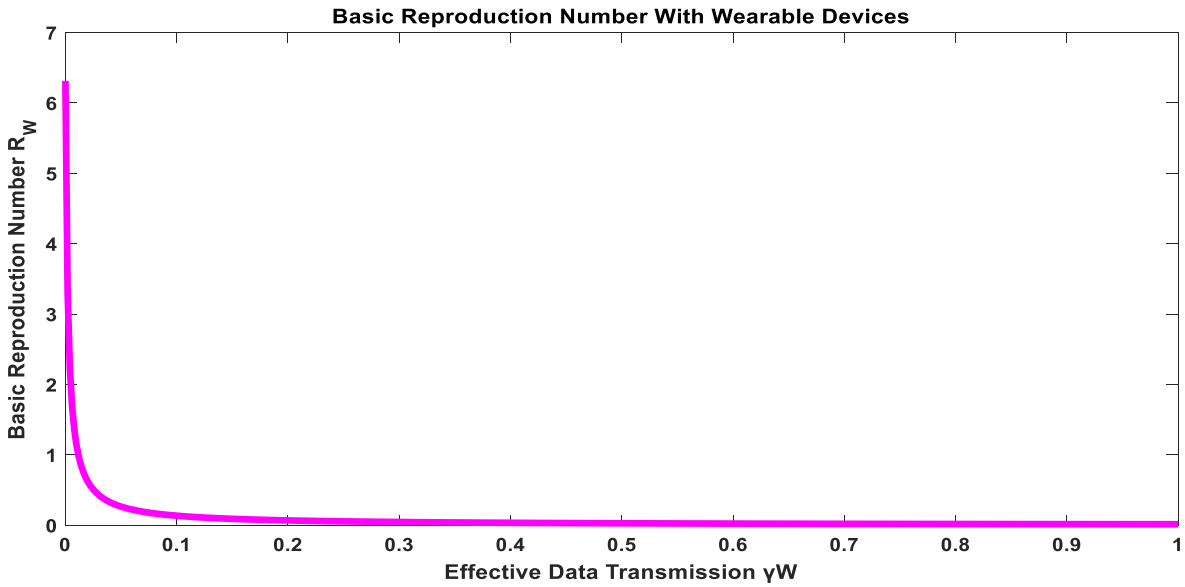

Fig. 2. Plot of basic reproduction number R_W of model (11) with WHMD.

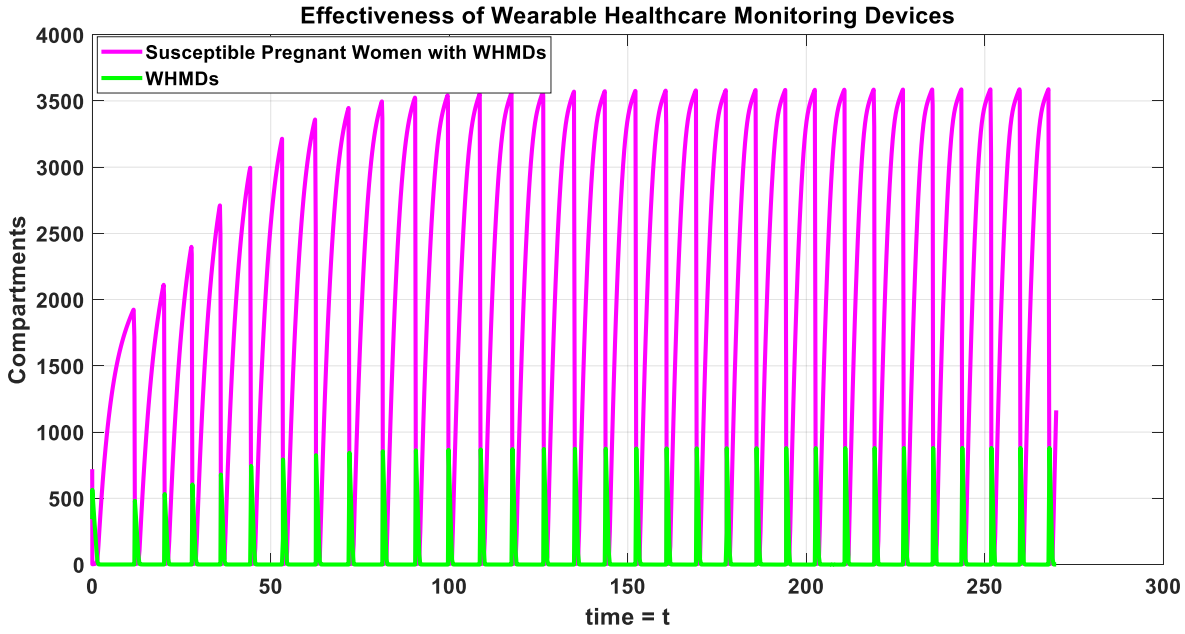

Fig. 3. Analytical behavior of Susceptible Pregnant patients with WHMD.

Fig. 5 illustrates the application of optimal control techniques for disease monitoring and prevention utilizing WHMD. In contrast, Fig. 6 portrays the dynamic behavior of pertinent variables when WHMDs are not employed by expectant mothers. In Fig. 4, the integration of wearables significantly enhances the well-being of pregnant patients. By promptly detecting health irregularities, these wearables facilitate proactive intervention. Moreover, these devices offer functionality to seamlessly share gathered health data with healthcare professionals. This data empowers care providers to recommend tailored measures that ameliorate the health of expectant mothers. Consequently, a notable decline in the count of pregnant patient susceptible to and afflicted by pregnancy-related ailments is observed. Conversely, Fig. 5 exhibits a rise in the number of exposed and infected pregnant patients, coinciding with the non-utilisation of wearable devices. Upholding the sustained functionality of these wearable devices, a judicious employment of low-energy protocols is instituted. This strategic energy management curtails the depletion rate of wearable devices. Evidently, Fig. 5 illustrates a diminishing population of wearable devices due to routine usage, while Fig. 6 demonstrates an incessant increase in device proliferation.

Figs. 8–10 present a comparative analysis of the efficacy of WHMDs in scenarios involving pregnant patients, contrasting their utilisation and non-utilisation. The adoption of WHMDs is correlated with a marked reduction in the count of pregnant patients subjected to exposure and subsequent infections, as depicted in Figs. 7 and 8, respectively. Conversely, this adoption contributes to an increase in the population of pregnant patients undergoing treatment and subsequently recovering, as evidenced in Figs. 9 and 10.

Using the optimal models developed for WHMD, this work is currently being applied to existing health monitoring systems. In this

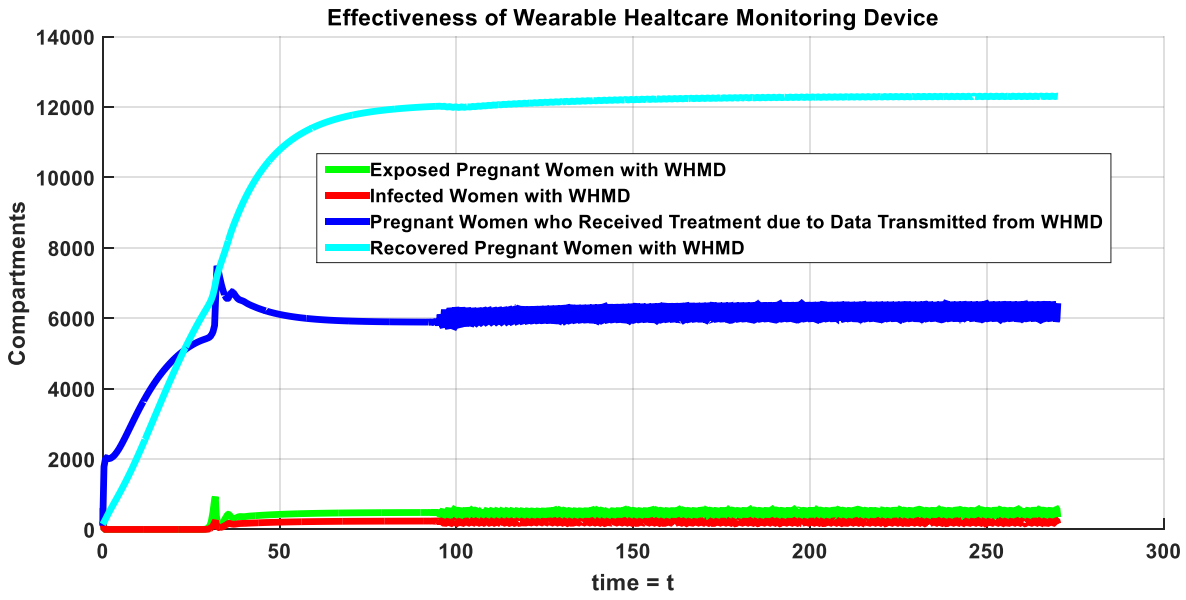

Fig. 4. Analytical behavior of the exposed, infected treated, and recovered Pregnant Patients with WHMD.

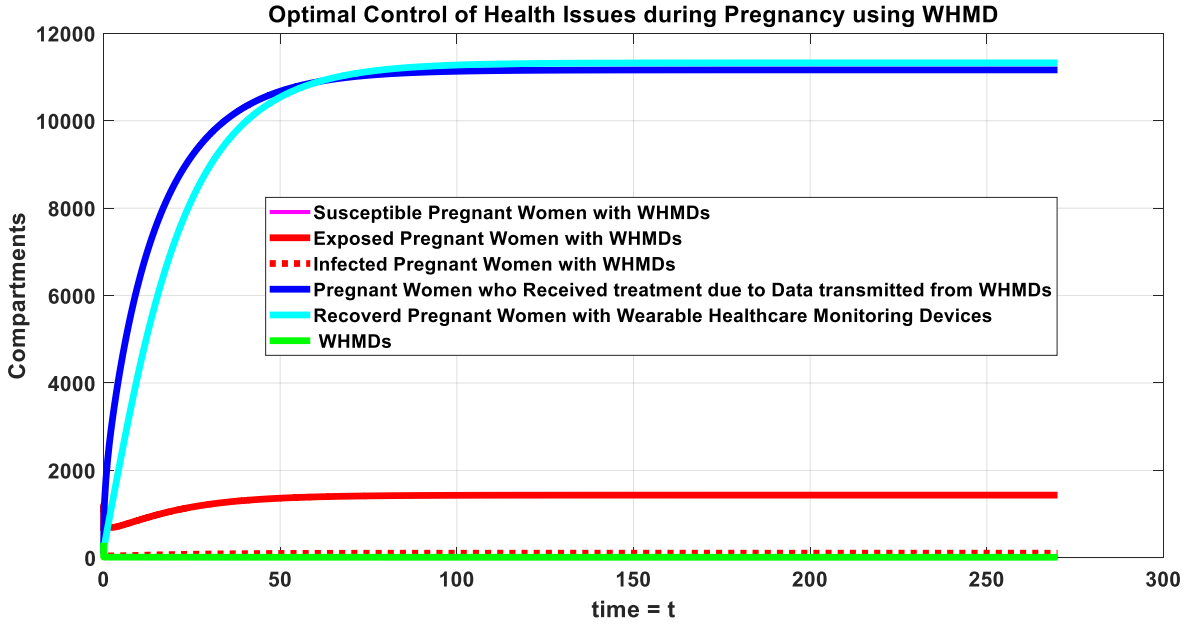

Fig. 5. Optimal control behavior of the compartments for Pregnant Patients with WHMD.

case, users can monitor their data in real time with a variety of health apps. For instance, Fitbit [44,45] tracks heart rate and physical activity; MyFitnessPal [46], tracks nutrition and exercise; Apple Health and Google Fit [47], integrate all health data. While some specialized applications, like Strava [48], concentrate on metrics related to cycling and running, others, like Sleep Cycle [49], examine sleep habits. Polar Flow [50] tracks heart rate and exercise, Garmin Connect syncs with wearables [51], Instant Blood Pressure uses a smartphone camera to assess blood pressure [52], and Cardiogram focuses on heart rate [53]. Real-time insights on various facets of health and wellness are provided by these apps. The absence of established computational model for these applications now offers an extended proof of concept for WHMD and its validations with machine learning algorithms in future research.

In the realm of telemedicine network routing, the paper [54] introduced the Energy Enhanced Threshold Routing Protocol (ETH--LEACH) as a novel approach aimed at overcoming limitations within traditional wireless sensor networks (WSNs), making them viable for potential telemedicine integration. Optimizing energy consumption through time division multiple access (TDMA) for path estimation could significantly augment the WHMD computational model. Another model [55] is capable of estimating the anticipated number of health issues considering confirmed cases, recoveries, deaths, and active cases in weeks. Metrics such as accuracy and error rates, along with Support Vector Machine, Logistic Regression, and Convolutional Neural Network models, demonstrate efficiency in predicting disease diffusion.

A machine learning model (MLM) [56] was deployed to assess COVID-19 risk in diabetic patients without medical practitioner intervention. This model, akin to the WHMD computational model, identified

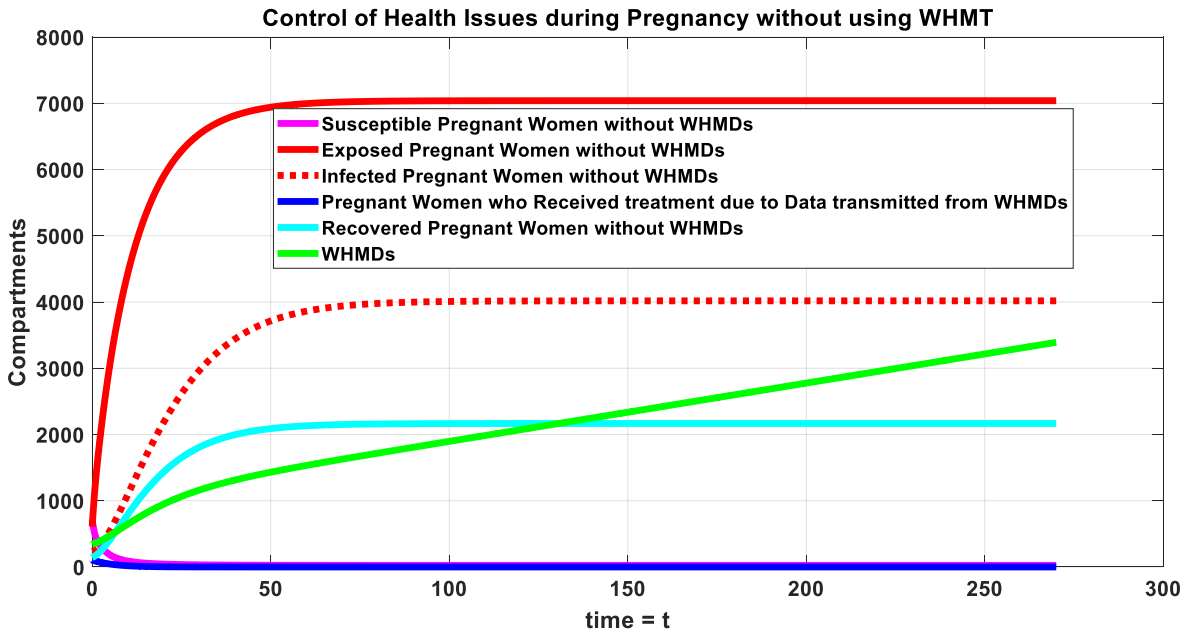

Fig. 6. Optimal control behavior among the compartments of Pregnant Patients without WHMDs.

eight influential symptoms in diabetic individuals through MLM. CatBoost classifier, logistic regression, and XGBoost were considered, ensuring the reliability of the developed model through hyper-parameter optimization for evaluating COVID-19 risk in diabetic patients.

Beyond the prerequisites of telemedicine routing, the studies [57,58] utilized a Dense Convolutional Neural Network (Dense-CNN) employing a novel cross-entropy-based loss function for enhanced COVID-19 patient classification in CT scans. Compared to existing methods, this work offered improved accuracy while reducing false negatives. This advancement can significantly enhance diagnosis within the WHMD computational model. Similarly, the study [59] concentrated on refining predictive analytics and data transmission in StreamRobot for internet of things (IoT) applications. It addressed vulnerabilities, node failures, and latency issues through edge system models, software-defined optimization, and resilient data transmission mechanisms. While these endeavors showcase enhanced reliability in remote monitoring utilizing advanced networking and predictive machine learning, resulting in improved data prediction accuracy and network scalability, the proposed WHMD analytical prediction model provides a more robust analytical framework specifically for telemedicine traffic workloads.

From the previous findings, important research directions have been highlighted below.

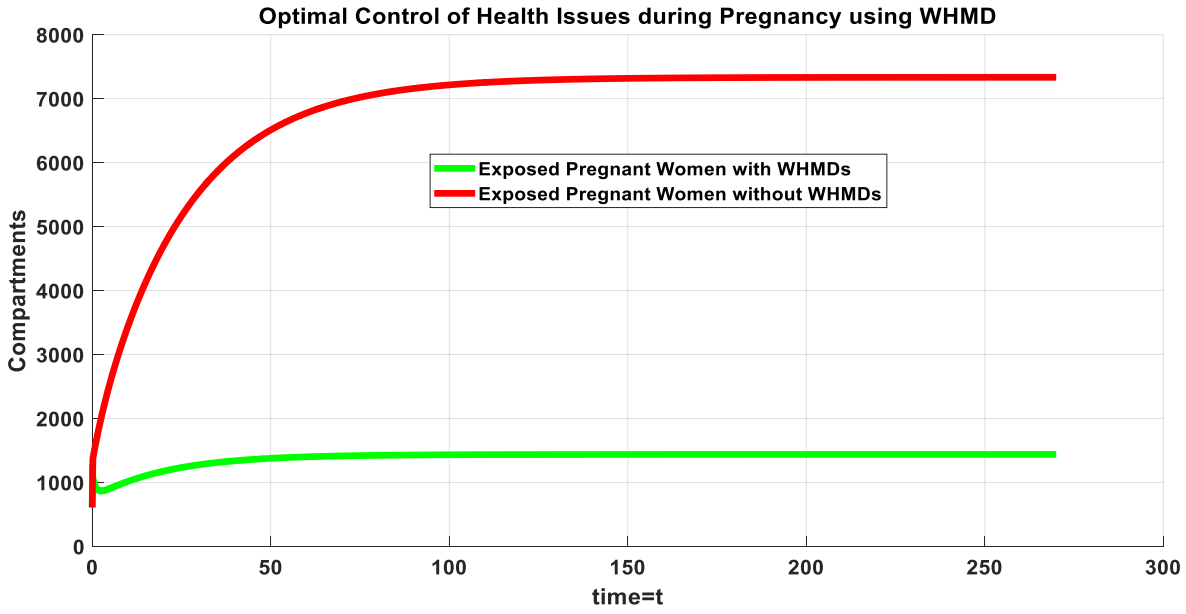

Fig. 7. Optimal control behavior of exposed Pregnant Patients with and without WHMDs.

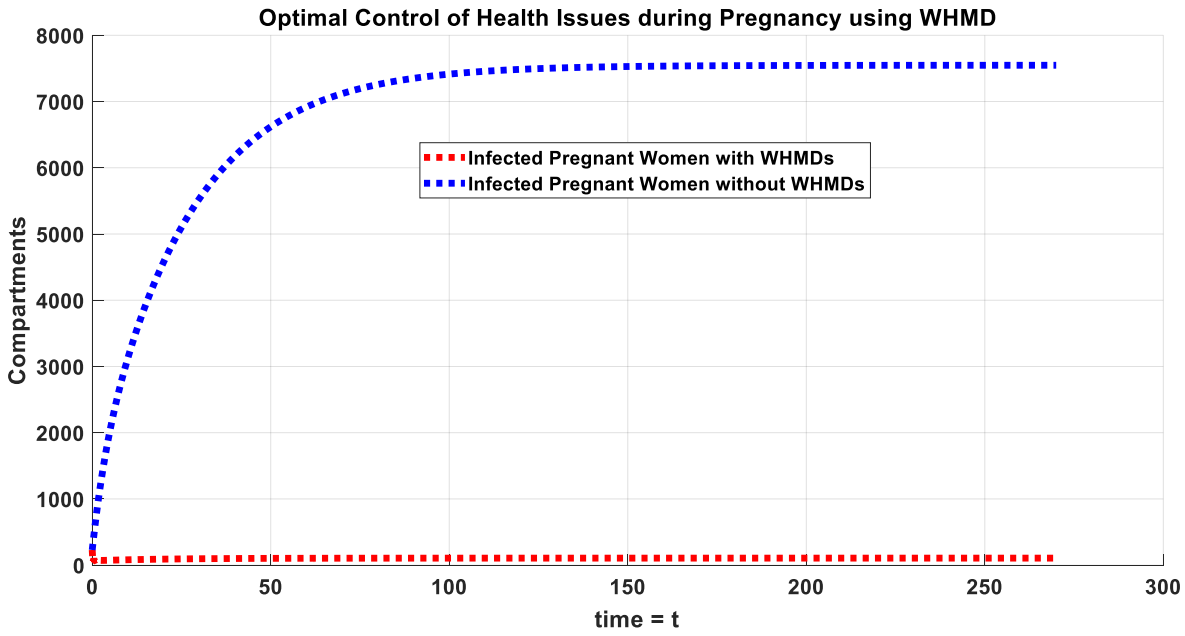

Fig. 8. Optimal control behavior of infected Pregnant Patients with and without WHMDs.

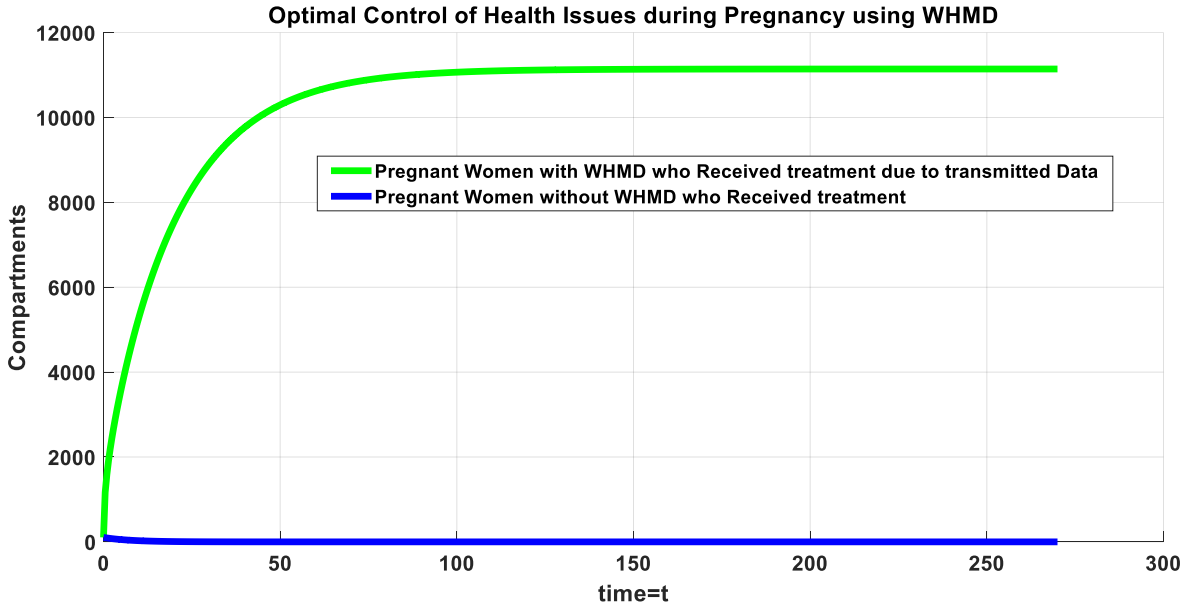

Fig. 9. Optimal control behavior of treated pregnant patients with and without WHMDs.

1. Integration of WHMD with Existing Health Monitoring Apps:
   - Explore the integration of WHMD computational models with popular health apps like Fitbit, MyFitnessPal, Apple Health, Google Fit, Strava, Sleep Cycle, Polar Flow, Garmin Connect, Instant Blood Pressure, Cardiogram, etc. This could involve creating interoperability or collaborative frameworks that leverage the strengths of both WHMD and these applications.
2. Enhancement of Telemedicine Network Routing:
   - Investigate further advancements in telemedicine network routing, potentially building on the Energy Enhanced Threshold Routing Protocol (ETH-LEACH) to optimize energy consumption. This could involve integrating WHMD computational models for more efficient data transmission from the edge networks.
3. Disease Prediction Models and Risk Assessment:
   - Expand on the machine learning models for predicting disease diffusion and assessing risk in specific populations (such as pregnant patients). Further research could involve refining these models, possibly incorporating more diverse data sources and advanced algorithms to improve accuracy and scalability.
4. Diagnostic Improvements Using Machine Learning:
   - Explore the integration of advanced machine learning techniques, like Dense Convolutional Neural Networks (Dense-CNN) applied to CT scans, within WHMD for improved diagnostic accuracy. This could involve refining and adapting these models specifically for WHMD applications.
5. IoT Applications for Remote Monitoring:
   - Investigate IoT applications for edge remote monitoring, focusing on predictive analytics, data transmission reliability, and network scalability. This research could involve incorporating WHMD

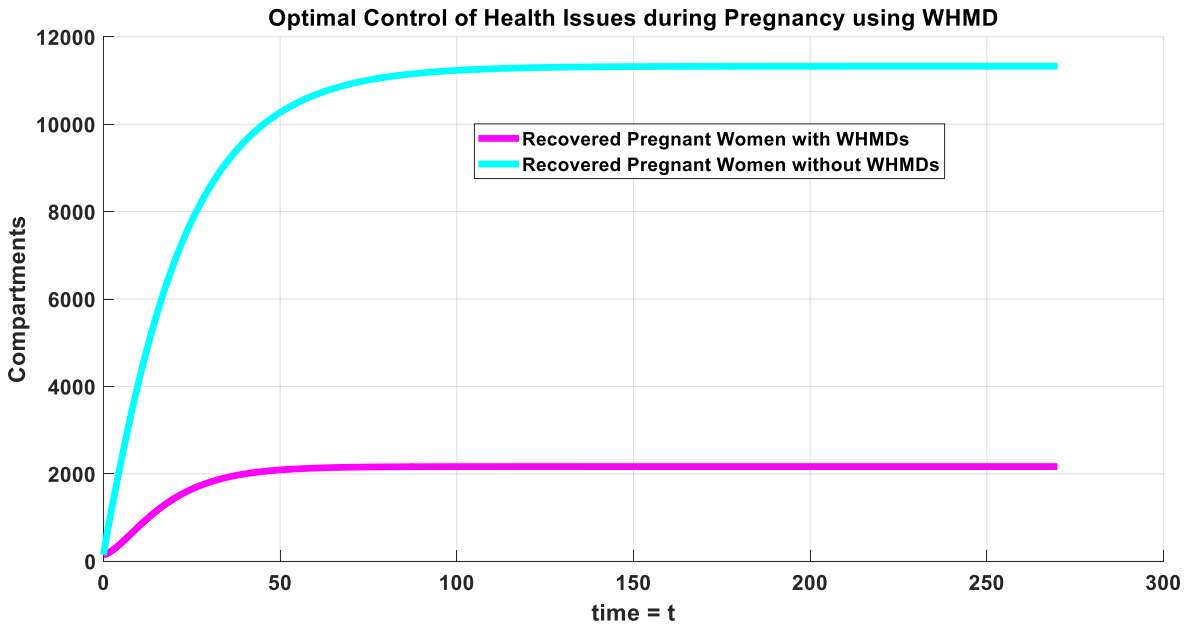

Fig. 10. Optimal control behavior of recovered pregnant patients with and without WHMD.

analytical prediction models to enhance the reliability and accuracy of predictive analytics in IoT-based health monitoring systems.

6. Robust Analytical Framework for Telemedicine Traffic Workloads:
   - Develop a more robust analytical framework specifically designed to handle telemedicine traffic workloads. This could involve refining existing models or creating new frameworks that specifically address the challenges and complexities of telemedicine data.

These directions showcase new opportunities that can potentially contribute to the advancement and application of WHMD in diverse healthcare and telemedicine contexts.

7. Conclusion

This paper presents the transformative potential of the Fractional-Order Multidimensional Telemedicine model (FMDTM) in addressing healthcare challenges for pregnant patients in underserved communities. The shift from traditional integer-order systems to fractional-order differential equations is not only theoretically promising but also practically advantageous. The WHMD model introduces a groundbreaking solution for proactive pregnancy care, monitoring vital health indicators and enabling informed decision-making for both healthcare providers and expecting mothers. This proactive approach allows anticipation and prediction of potential health issues, reducing complications and contributing to stabilized health management. The analysis of the basic reproduction number demonstrates that WHMDs effectively control health imbalances during pregnancy, leading to a reduction in new disease cases. The integration of WHMDs into pregnancy care significantly reduces exposure and infections while increasing treatment and recovery rates. This shift from reactive to proactive healthcare improves overall health outcomes for pregnant individuals, potentially reducing hospitalizations and suffering. The research suggests wearable devices can predict diseases before escalation, offering a crucial window for timely intervention. Furthermore, future research will investigate into the experimental application of machine learning techniques for WHMD analytics.

Finally, the combination of fractional-order modeling and WHMDs presents a promising trajectory for the future of pregnancy care, particularly in underserved communities, emphasizing the potential societal impact of proactive, personalized, and preventative healthcare.

Declaration of competing interest

* None of the authors of this paper has a financial or personal relationship with other people or organizations that could inappropriately influence or bias the content of the paper.
* It is to specifically state that "No Competing interests are at stake and there is No Conflict of Interest" with other people or organizations that could inappropriately influence or bias the content of the paper.

Data availability

Data will be made available on request.

Acknowledgments

This research is partly sponsored by Nigeria Tertiary Education Fund under the grant number TETF/ES/UNIV/IMO STATE/TSAS/2021 with supports from Smart innovation Infrastructure & Industry research group, Manchester Metropolitan University, UK.

References

[1] R. Ghosh, S. Sarkhel, P. Saha, MoS2-Based dual-gate mosfet as ultrasensitive SARs-CoV-2 biosensor for rapid screening of respiratory syndrome, IEEE Sensors Letters 7 (11) (Nov. 2023) 1–4, https://doi.org/10.1109/LSENS.2023.3321012. Art no. 4503304.

[2] L. Abirami, J. Karthikeyan, Digital twin-based healthcare system (DTHS) for earlier Parkinson disease identification and diagnosis using optimized fuzzy based k-nearest neighbor classifier model, IEEE Access 11 (2023) 96661–96672, https://doi.org/10.1109/ACCESS.2023.3312278.

[3] S. Hiremath, G. Yang, K. Mankodiya, Wearable Internet of Things: concept, architectural components and promises for person-centered healthcare, in: 2014 4th International Conference on Wireless Mobile Communication and Healthcare - Transforming Healthcare through Innovations in Mobile and Wireless Technologies (MOBIHEALTH), 2014, pp. 304–307, https://doi.org/10.1109/MOBIHEALTH.2014.7015971. Athens, Greece.

[4] G.V. Aiosa, M. Palesi, F. Sapuppo, EXplainable AI for decision Support to obesity comorbidities diagnosis, IEEE Access 11 (2023) 107767–107782, https://doi.org/10.1109/ACCESS.2023.3320057.

[5] J. Mišeikis, et al., Lio-A personal robot assistant for human-robot interaction and care applications, IEEE Rob. Autom. Lett. 5 (4) (Oct. 2020) 5339–5346, https://doi.org/10.1109/LRA.2020.3007462.

[6] IEEE Draft Standard for a Smart Transducer Interface for Sensors, Actuators, Devices, and Systems - Common Functions, Communication Protocols, and Transducer Electronic Data Sheet (TEDS) Formats, IEEE P1451.0/D7, 2 Nov. 2023, pp. 1–442. October 2023.
[7] A. Ahmed, R. Xi, M. Hou, S.A. Shah, S. Hameed, Harnessing big data analytics for healthcare: a comprehensive review of frameworks, implications, applications, and impacts, IEEE Access 11 (2023) 112891–112928, https://doi.org/10.1109/ACCESS.2023.3323574.
[8] K.C. Okafor, O.M. Longe, WearROBOT: an energy conservative wearable obstacle detection robot with LP multi-commodity graph, IEEE Access 10 (2022) 105843–105865, https://doi.org/10.1109/ACCESS.2022.3211319.
[9] Jing Zhang, Fangman Chen, Yongli Wang, Yahong Chen, Early detection and prediction of acute exacerbation of chronic obstructive pulmonary disease, Chinese Medical Journal Pulmonary and Critical Care Medicine 1 (2) (2023) 102–107.
[10] E. Paul, Diwas KC. George, Morgan Greenleaf, Jay Shah, Wilbur A. Lam, C. Matthew hawkins, bridging the divide: unintended consequences of the shift to home-based telemedicine, J. Pediatr. (2023), https://doi.org/10.1016/j.jpeds.2023.113719.
[11] William Mualem, SulamanDurrani, Nikita Lakomkin, Jamie Van Gompel, MohamadBydon Alfredo Quiñones-Hinojosa, Utilizing data from wearable technologies in the era of telemedicine to assess patient function and outcomes in neurosurgery: systematic review and time-trend analysis of the literature, World Neurosurgery 166 (2022) 90–119, https://doi.org/10.1016/j.wneu.2022.07.036.
[12] ShadabFaham, AbdollahSalimi, RaoufGhavami, Electrochemical-based remote biomarker monitoring: toward internet of wearable things in telemedicine, Talanta 253 (2023), https://doi.org/10.1016/j.talanta.2022.123892.
[13] Temitayo A. Akosile, B. Dholaria, Nasima Mehraban, Brittney Baer, N. Long, R. Jayani, A. Kassim, B. Engelhardt, S. Sengsayadeth, Vivek G. Patel, Shakthi T Bhaskar, B. Savani, Olalekan O. Oluwole, 201 - the impact of telemedicine and wearable devices in improving the safety profile of outpatient chimeric antigen receptor T-Cell (CAR-T) therapies: a case-control study, Transplantation and Cellular Therapy 29 (2) (2023), https://doi.org/10.1016/S2666-6367(23)00270-1. Supplement.
[14] Shah Jahan PoojaYadav, Kamal Shah, Olumuyiwa James Peter, ThabetAbdeljawad, "Fractional-order modelling and analysis of diabetes mellitus: utilizing the Atangana-Baleanu Caputo (ABC) operator, Alex. Eng. J. 81 (2023) 200–209, https://doi.org/10.1016/j.aej.2023.09.006.
[15] Jingwen Zhang, Yize Zhou, Zhigang Wang, Haohua Wang, Analysis and achievement for fractional optimal control of Hepatitis B with Caputo operator, Alex. Eng. J. 70 (2023), https://doi.org/10.1016/j.aej.2023.03.015.
[16] Tingsong Du, Yu Peng, Hermite–Hadamard type inequalities for multiplicative Riemann–Liouville fractional integrals, J. Comput. Appl. Math. (2023), https://doi.org/10.1016/j.cam.2023.115582.
[17] J.O. Akanni, F.O. Akinpelu, S. Olaniyi, A.T. Oladipo, A.W. Ogunsola, Modeling financial crime population dynamics: optimal control and cost-effectiveness analysis, International Journal of Dynamics, and Control 8 (2020) 531–544, https://doi.org/10.1007/s40435-019-00572-3.
[18] H.T. Alemneh, Mathematical modeling, analysis, and optimal control of corruption dynamics, J. Appl. Math. 13 (2020) 5109841, https://doi.org/10.1155/2020/5109841.
[19] C. Castillo-Chavez, Z. Feng, W. Huang, On the computation of R0 and its role on global stability, Mathematical Approaches for Emerging and Reemerging Infectious Diseases: An Introduction 1 (2002) 229–250, https://doi.org/10.1007/978-1-4757-3667-013. Springer.
[20] Adesoye Idowu Abioye, Olumuyiwa James Peter, Hammed Abiodun Ogunseye, Festus Abiodun Oguntolu, Tawakalt Abosede Ayoola, Asimiyu Olalekan Oladapo, A fractional-order mathematical model for malaria and COVID-19 co-infection dynamics, Healthcare Analytics 4 (2023), https://doi.org/10.1016/j.health.2023.100210.
[21] Saima Rashid, Fahd Jarad, Abdulaziz Khalid Alsharidi, Numerical investigation of fractional-order cholera epidemic model with transmission dynamics via fractal–fractional operator technique, Chaos, Solit. Fractals 162 (2022), https://doi.org/10.1016/j.chaos.2022.112477.
[22] Ayub Khan, Lone Seth Jahanzaib, PushaliTrikha, "secure communication: using parallel synchronization technique on novel fractional order chaotic system, IFAC-PapersOnLine 53 (1) (2020) 307–312, https://doi.org/10.1016/j.ifacol.2020.06.052.
[23] Jean-Francois Mangin, Denis Rivière, Edouard Duchesnay, Yann Cointepas, Véronique Gaura, Christophe Verny, Philippe Damier, Pierre Krystkowiak, Bachoud-Lévi Anne-Catherine, Philippe Hantraye, Philippe Remy, Gwenaëlle Douaud, Neocortical morphometry in Huntington's disease: indication of the coexistence of abnormal neurodevelopmental and neurodegenerative processes, Neuroimage: Clinical 26 (2020), https://doi.org/10.1016/j.nicl.2020.102211.
[24] Kanwalpreet Kaur, Neeru Jindal, Kulbir Singh, "QRFODD: Quaternion Riesz fractional order directional derivative for color image edge detection,", Signal Process., Vol. 212. https://doi.org/10.1016/j.sigpro.2023.109170.
[25] Muhammad Farman, Ali Akgül AamirShehzad, NourhaneAttia DumitruBaleanu, Ahmed M. Hassan, Analysis of a fractional order Bovine Brucellosis disease model with discrete generalized Mittag–Leffler kernels, Results Phys. 52 (2023), https://doi.org/10.1016/j.rinp.2023.106887.
[26] A.A. Adeniji, O.A. Mogbojuri, M.C. Kekana, S.E. Fadugba, Numerical solution of rotavirus model using Runge-Kutta-Fehlberg method, differential transform method and Laplace Adomian decomposition method, Alex. Eng. J. 82 (2023), https://doi.org/10.1016/j.aej.2023.10.001.
[27] Pshtiwan Othman Mohammed MusawaYahyaAlmusawa, Approximation of sequential fractional systems of Liouville–Caputo type by discrete delta difference operators, Chaos, Solit. Fractals 176 (2023), https://doi.org/10.1016/j.chaos.2023.114098.
[28] O.M. Ogunmiloro, Mathematical analysis and approximate solution of a fractional order Caputo fasciolíasis disease model, Chaos, Solitons and Fractals 146 (2021) 110851, https://doi.org/10.1016/j.chaos.2021.110851.
[29] Testa Alexander, Jacqueline Diaz, Kyle T. Ganson, Dylan B. Jackson, Jason M. Nagata, Maternal disability and prenatal oral health experiences: findings from pregnancy risk assessment monitoring system, J. Am. Dent. Assoc. 154 (3) (2023), https://doi.org/10.1016/j.adaj.2022.11.018. Ppg. 225-234.e7.
[30] C.P. Li, Y.T. Ma, Fractional dynamical system and its linearization theorem, Nonlinear Dynam. 71 (2013) 621–633, https://doi.org/10.1007/s11071-012-0601-1.
[31] Z. Alkhudhari, S. Al-Sheikh, S. Al-Tuwairqi, Global dynamics of a mathematical model on smoking, Appl. Math. 1 (2014) 847075, https://doi.org/10.1155/2014/847075.
[32] O.M. Ogunmiloro, A.S. Idowu, T.O. Ogunlade, R.O. Akindutire, On the mathematical modeling of measles disease dynamics with encephalitis and relapse under the atangana-baleanu-caputo fractional operator and real measles data of Nigeria, Int. J. Appl. Comput. Math. 7 (2021) 1–20, https://doi.org/10.1007/s40819-021-01122-2.
[33] O.M. Mirza, H. Mujlid, H. Manoharan, S. Selvarajan, G. Srivastava, M.A. Khan, Mathematical framework for wearable devices in the internet of things using deep learning, Diagnostics 12 (2022) 2750, https://doi.org/10.3390/diagnostics12112750.
[34] P. Van den Driessche, J. Watmough, Reproduction numbers and sub-threshold endemic equilibrium for compartmental models of disease transmission, Math. Biosci. 180 (2002) 28–29.
[35] O. Diekmann, J.A.P. Heesterbeek, J.A. Metz, On the definition and the computation of the basic reproduction ratio R_0 in models for infectious diseases in heterogeneous populations, J. Math. Biol. 28 (1990) 365–382.
[36] N.H. weilam, S.M. Al-Mekhlafi, "On the optimal control for fractional multi-strain TB model," Optim, Control Appl. Methods 37 (6) (2016) 1355–1374, https://doi.org/10.1002/oca.2247 [Online]. Available:.
[37] O.P. Agrawal, On a general formulation for the numerical solution of optimal control problems, Int. J. Control 28 (1–4) (2004) 323–337.
[38] O.P. Agrawal, Formulation of Euler–Lagrange equations for fractional variational problems, J. Math. Anal. Appl. 272 (1) (2002) 368–379.
[39] O.P. Agrawal, A formulation and numerical scheme for fractional optimal control problems, IFAC Proc 39 (11) (2006) 68–72.
[40] O.P. Agrawal, O. Defterli, D. Baleanu, Fractional optimal control problems with several state and control variables, J. Vib. Control 16 (13) (2010) 1967–1976.
[41] W.H. Fleming, R.W. Rishel, Deterministic and Stochastic Optimal Control, Springer, New York, 1975.
[42] D.L. Lukes, Differential equations: classical to controlled, Math. Sci. Eng. 162 (1982). Academic Press, New York.
[43] F. Ndairou, I. Area, J.J. Niet, C.J. Silva, D.F. Torrees M, Mathematical modeling of Zika disease in pregnant women and newborn with microcephaly in Brazil, Math. Method Appl. Sci. 41 (18) (2017) 8929–8941. ISSN 0170-4214.
[44] J. Zhou, Differential Transformation and its Applications for Electrical Circuits, Gal Eylon, LiatTikotzky, IlanDinstein, "Performance evaluation of Fitbit Charge 3 and actigraphy vs. polysomnography: Sensitivity, specificity, and reliability across participants and nights, Sleep Health, Huazhong University Press, Wuhan, China, 1986, pp. 407–416, https://doi.org/10.1016/j.sleh.2023.04.001, 9(4) 2023.
[45] Megan McMahon, Isabella McConley, Chand Hashim, M. David, Schnyer, Fitbit validation for rest-activity rhythm assessment in young and older adults, Smart Health 29 (2023), https://doi.org/10.1016/j.smhl.2023.100418.
[46] Chloe Lozano, John Apolzan, Stephanie Broyles, Corby Martin, SanjoySaha, P31-078-23 validity of the portion size and MyFitnessPal mobile apps for estimating energy intake by demographic characteristics: a randomized laboratory-based evaluation, Curr. Dev. Nutr. 7 (1) (2023), https://doi.org/10.1016/j.cdnut.2023.101643.
[47] Sara Sabri Samara AshokanArumugam, Reime Jamal Shalash, Raneen Mohammed Qadah, AmnaMajidFarhani, Hawra Mohammed Alnajim, Hanan Youssef Alkalih, Does Google Fit provide valid energy expenditure measurements of functional tasks compared to those of Fibion accelerometer in healthy individuals? A cross-sectional study, Diabetes Metabol. Syndr.: Clin. Res. Rev. 15 (6) (2021), https://doi.org/10.1016/j.dsx.2021.102301.
[48] Gilles Jean-Louis, Michelle Eckhardt, Simone Podschun, Judith Mahnkopf, Markus Venohr, Estimating daily bicycle counts with Strava data in rural and urban locations, Travel Behaviour and Society 34 (2024), https://doi.org/10.1016/j.tbs.2023.100694.
[49] Sleep Cycle, "Sleep Cycle | Sleep Tracker, Monitor & Alarm Clock," Sleep Cycle, https://www.sleepcycle.com. Accessed: November 6, 2023.
[50] Polar Electro Oy, "Polar Flow," Polar Flow, https://flow.polar.com. Accessed: November 6, 2023.
[51] Fabian Nunes, PatrícioDomingues, Miguel Frade, Post-mortem digital forensic analysis of the Garmin Connect application for Android, Forensic Sci. Int.: Digit. Invest. 47 (2023), https://doi.org/10.1016/j.fsidi.2023.301624.
[52] Instant Blood Pressure, https://www.instantbloodpressure.com. Accessed: November 6, 2023.
[53] Cardiogram, Inc., "Cardiogram: Heart Rate Monitor," Version 12+, App Store, https://apps.apple.com/us/app/cardiogram-heart-rate-monitor/id1000017994. Accessed: November 6, 2023.

[54] P.K. Chithaluru, M.S. Khan, M. Kumar, T. Stephan, ETH-LEACH: an energy enhanced threshold routing protocol for WSNs, Int. J. Commun. Syst. (2021), https://doi.org/10.1002/dac.4881.

[55] S. Raheja, S. Kasturia, X. Cheng, et al., Machine learning-based diffusion model for prediction of coronavirus-19 outbreak, Neural Comput. Appl. 35 (2023) 13755–13774, https://doi.org/10.1007/s00521-021-06376-x.

[56] A. Aggarwal, M. Chakradar, M.S. Bhatia, M. Kumar, T. Stephan, S.K. Gupta, S. H. Alsamhi, H. Al-Dois, COVID-19 risk prediction for diabetic patients using fuzzy inference system and machine learning approaches, J Healthc Eng (2022 Apr 1; 2022) 4096950, https://doi.org/10.1155/2022/4096950. .PMID: 35368915; PMCID: PMC8974235.

[57] Motwani Anand, Piyush Kumar Shukla, Mahesh Pawar, Manoj Kumar, Uttam Ghosh, Waleed Alnumay, Soumya Ranjan Nayak, Enhanced framework for COVID-19 prediction with computed tomography scan images using dense convolutional neural network and novel loss function, Comput. Electr. Eng. 105 (2023).

[58] Santosh Kumar, Sachin Kumar Gupta, Vinit Kumar, Manoj Kumar, Mithilesh Kumar Chaube, Nenavath Srinivas Naik, Ensemble multimodal deep learning for early diagnosis and accurate classification of COVID-19, Comput. Electr. Eng. 103 (2022).

[59] Kennedy Chinedu Okafor, Omowunmi Mary Longe, Smart deployment of IoT-TelosB service care StreamRobot using software-defined reliability optimisation design, Heliyon 8 (Issue 6) (2022).

[60] R. Mcconkey, O. Olukoya, Runtime and design time completeness checking of dangerous android app permissions against GDPR, IEEE Access 12 (2024) 1–22, https://doi.org/10.1109/ACCESS.2023.3347194.